Stability Analysis of Social Foraging Swarms

Veysel Gazi, *Member, IEEE,* and Kevin M. Passino, *Senior Member, IEEE*

***Abstract*—In this article we specify an M-member "individual-based" continuous time swarm model with individuals that move in an n-dimensional space according to an attractant/repellent or a nutrient profile. The motion of each individual is determined by three factors: i) attraction to the other individuals on long distances; ii) repulsion from the other individuals on short distances; and iii) attraction to the more favorable regions (or repulsion from the unfavorable regions) of the attractant/repellent profile. The emergent behavior of the swarm motion is the result of a balance between inter-individual interactions and the simultaneous interactions of the swarm members with their environment. We study the stability properties of the collective behavior of the swarm for different profiles and provide conditions for collective convergence to more favorable regions of the profile.**

***Index Terms*—Aggregations, attraction, continuous time swarm, gradient climbing, individual-based, inter-individual interactions, multi-agent systems, n-dimensional space, repulsion, stability analysis, swarms.**

I. Introduction

SWARMING, or aggregations of organizms in groups, can be found in nature in many organizms ranging from simple bacteria to mammals. Such behavior can result from several different mechanisms. For example, individuals may respond directly to local physical cues such as concentration of nutrients or distribution of some chemicals (which may be laid by other individuals). This process is called *chemotaxis* and is used by organizms such as bacteria or social insects (e.g., by ants in trail following or by honey bees in cluster formation). As another example, individuals may respond directly to other individuals (rather than the cues they leave about their activities) as seen in some higher organizms such as fish, birds, and herds of mammals.

Evolution of swarming behavior is driven by the advantages of such collective and coordinated behavior for avoiding predators and increasing the chance of finding food. For example, in [1], [2] Grünbaum explains how social foragers as a group more successfully perform chemotaxis over noisy gradients than individually. In other words, individuals do much better collectively compared to the case when they forage on their own. Operational principles from such biological systems can be used in engineering for developing distributed cooperative control, coordination, and learning strategies for autonomous multi-agent systems such as autonomous multi-robot applications, unmanned undersea, land, or air vehicles. The development of such highly automated systems is likely to benefit from biological principles including modeling of biological swarms, coordination strategy specification, and analysis to show that group dynamics achieve group goals. In this article we develop a simple model of swarming in the presence of an attractant/repellent or a nutrient profile and analyze its stability properties for different profiles. We show collective convergence to more favorable regions of the profile. The model that we develop here can be viewed as a representation of cohesive social foraging of swarms.

Biologists have been working on understanding and modeling of swarming behavior for a long time [3]–[9]. There are two fundamentally different approaches that they have been considering for analysis of swarm dynamics. These are *spatial* and *nonspatial* approaches. In the spatial approach the space (environment) is either explicitly or implicitly present in the model and the analysis. It can be divided into two distinct frameworks which are *individual-based* (or Lagrangian) framework and *continuum* (or Eulerian) framework [6]. In the individual-based models the basic description is the motion equation of each (separate) individual and therefore it is a natural approach for modeling and analysis of complex social interactions and aggregations. The general understanding within this framework now is that the swarming behavior is a result of an interplay between a long range attraction and a short range repulsion between the individuals. The work by Breder in [3], where he suggested a simple model composed of a constant attraction term and a repulsion term which is inversely proportional to the square of the distance between two members is one of the early works within this framework. Similarly, in [4] Warburton and Lazarus also considered an individual-based swarm model and studied the effect on cohesion of a family of attraction/repulsion functions.

In the Eulerian framework the swarm dynamics are described using a *continuum model* of the *flux*, namely *concentration* or *population density* (i.e., a model in which each member of the swarm is not considered as individual entity, but the swarm is a continuum described by its density in one, two, or three dimensional space) described by partial differential equations of the swarm density. The basic equation of the Eulerian models is the *advection-diffusion-reaction* equation, where advection and diffusion are the joint outcome of individual behavior and environmental influences, and the reaction term is due to the population dynamics. See, for example, [7] where the authors

Manuscript received December 24, 2002; revised June 3, 2003. This work was supported by the DARPA MICA program via the AFRL under Contract F33615-01-C-3151 and TÜBİTAK (the Scientific and Technical Research Council of Turkey). This paper was recommended by Associate Editor D. Cook.

V. Gazi was with the Department of Electrical Engineering, Ohio State University, Columbus, OH 43210 USA. He is now with the Department of Electrical and Electronics Engineering, Atilim University, Ankara 06836, Turkey (e-mail: veysel_gazi@atilim.edu.tr).

K. M. Passino is with the Department of Electrical Engineering, Ohio State University, Columbus, OH 43210 USA (e-mail: passino. 1@osu.edu).

Digital Object Identifier 10.1109/TSMCB.2003.817077

present a swarm model which is based on nonlocal interactions of the swarm members. Their model consists of integro-differential advection-diffusion equations with convolution terms that describe attraction and repulsion.

In the nonspatial approaches the population level swarming dynamics are described in a nonspatial way in terms of frequency distributions of groups of various size. It is assumed that groups of various sizes split or merge into other groups based on the inherent group dynamics, environmental conditions, and encounters of other groups. See, for example, [9] where the authors present a general continuous model for animal group size distribution (a nonspatial patch model). They consider a population with fixed size that is divided into groups of various dynamic sizes. The drawback of the nonspatial approaches is that they need several "artificial" assumptions about fusion and fission of groups of various sizes in order to describe and analyze the population dynamics.

Each of the above approaches has its advantages and disadvantages. A comparative study is presented by Durrett and Levin in [8], where they compare four different approaches to modeling the dynamics of spatially distributed systems by using three different examples, each with different realistic biological assumptions. They show that the solutions of all the models do not always agree, and argue in favor of the discrete (individual based) models that treat the space explicitly. In a recent study in [10] Parrish and her colleagues survey similarities and differences between different models of swarm aggregations and present preliminary results of efforts to unify all the models within a single framework. A good background and a review of the swarm modeling concepts and literature such as spatial and nonspatial models, individual-based versus continuum models and so on can be found in [5] and [6]. See also [11] and [12] and references therein for other related work. Other general references are the books by Edelshtein–Keshet [13] and Murray [14].

In parallel to the mathematical biologists there are a number of physicists who have done important work on swarming behavior [15]–[20]. The general approach the physicists take is to model each individual as a particle and study the collective behavior due to their interaction. Many of them assume that particles are moving with constant absolute velocity and at each time step each one travels in the average direction of motion of the particles in its neighborhood with some random perturbation. They try to study the affect of the noise on the collective behavior and to validate their models through extensive simulations.

For many organizms, swarming often occurs during "social foraging" and with the focus in this paper on studying the interactions between inter-individual cohesion mechanisms coupled with effects from the environment, particularly the attractant/repellent or nutrient profiles, there are other areas of relevant study. First, note that foraging theory is described in [21]. The recently popular "ant colony optimization" is an optimization method based on foraging in ant colonies and is discussed in [22]. There, the focus is on biomimicry for the solution of combinatorial optimization algorithms (e.g., shortest path algorithms) and swarming as we study it here is not considered. In [23] the author shows that chemotactic behavior of *E. coli* coupled with evolutionary and "elimination/dispersal events" provides for a nongradient distributed and parallel optimization procedure that can be used for adaptive control and cooperative control problems. Also, the author there used a similar characterization of an "attractant-repellent profile" to ours, and also studied swarm behavior as a distributed optimization method. Member-member swarming mechanisms are different from here, and are only considered from an optimization perspective. Stability analysis was not considered in [22], [23]. Another optimization method based on swarming behavior is the *particle swarm optimization* method [24], [25]. Although still there is no rigorous stability proof for its operation, it seems that it is a very effective method in function minimization.

In recent years, engineering applications such as formation control of multi-robot teams and autonomous air vehicles have emerged and this has increased the interest of engineers in swarms. Some examples include [26]–[28], where the authors describe formation control strategies for autonomous air vehicles and multiple autonomous land vehicle teams, respectively. Similar work includes the study of asynchronous distributed control and geometric pattern formation of multiple anonymous (or identical) robots [29] and the study on cooperative control and coordination of a group of holonomic mobile robots to capture/enclose a target by making group formations [30]. Another related approach is the *social potential fields* method for distributed control of groups of robots considered by Reif and Wang in [31]. It is based on artificial force laws between individual robots and robot groups, where the force laws are inverse-power or spring force laws incorporating both attraction and repulsion. It is an interesting and important work. However, it does not contain stability proof of the approach.

Other work on formation control and coordination of multiagent (multi-robot) teams can be found in [32]–[36]. In [32] a feedback linearization technique using only local information for controller design to exponentially stabilize the relative distances of the robots in the formation is proposed. Similarly, in [33], [34], the concept of control Lyapunov functions together with formation constraints is used to develop a formation control strategy and prove stability of the formation (i.e., formation maintenance). The results in [35], on the other hand, are based on using virtual leaders and artificial potentials for robot interactions in a group of agents for maintenance of the group geometry. By using the system kinetic energy and the artificial potential energy as a Lyapunov function closed loop stability is proved. Moreover, a dissipative term is employed in order to achieve asymptotic stability of the formation. In [36], the results in [35] are extended to the case in which the group is moving in a sampled gradient field.

Important work on swarm stability is given by Beni and coworkers in [37] and [38]. In [37] they consider a synchronous distributed control method for discrete one and two dimensional swarm structures and prove stability in the presence of disturbances using Lyapunov methods. On the other hand, [38] is, to best of our knowledge, one of the first stability results for asynchronous methods (with no time delays). There they consider a *linear* swarm model and provide sufficient conditions for the asynchronous convergence of the swarm to a synchronously achievable configuration.

Swarm stability under *total asynchronism* (i.e., asynchronism with time delays) was first considered in [39]–[41]. In [39] a one dimensional discrete time totally asynchronous swarm model is proposed and stability (swarm cohesion) is proved. The authors prove asymptotic convergence under total asynchronism conditions and finite time convergence under *partial asynchronism* conditions (i.e., total asynchronism with a bound on the maximum possible time delay). In [40], on the other hand, the authors consider a mobile swarm model and prove that cohesion will be preserved during motion under certain conditions, expressed as bounds on the maximum possible time delay. In [42] we obtained similar results to those in [39] for a swarm with a different mathematical model for the inter-member interactions and motions using some earlier results developed for parallel and distributed computation in computer networks in [43]. All of these stability investigations have been limited to either one or two dimensional space. Note that in one dimension, the problem of swarming is very similar to the problem of *platooning* of vehicles in *automated highway systems*, an area that has been studied extensively (see, for example, [44]–[46] and references therein).

Recently some results on the multidimensional case have been also obtained. For example, the work in [47], [48] is focusing on extending the work in [39]–[41] to the multidimensional case by imposing special constraints on the "leader" movements and by using a specific communication topology.

In [49], [50] we developed an "individual-based" continuous time synchronous model for swarm aggregations in n-dimensional space. We showed that for the given model the individuals will form a cohesive swarm in a finite time, and we obtained an explicit bound on the swarm size. In [51] we extended our results in [49], [50] to a more general class of attraction/repulsion functions and allowed for unbounded repulsion for collision avoidance. Note that in [49], [50], and [51] the motion of the swarm members was based only on inter-individual interactions and was not affected by the environment. In this article we build on our earlier results in [49]–[51] by considering a swarm which moves in an attractant/repellent profile (i.e., a profile of nutrients or toxic substances) and show collective convergence to (divergence from) more favorable (unfavorable) regions of the profile. The inter-individual interactions and the interactions with the environment in our model are based on *artificial potential functions*, a concept that has been used extensively for robot navigation and control [52], [53]. Therefore, our model here can be viewed as a type of a social potential fields model similar to the one in [31] (where no rigorous stability was considered). Therefore, the results here are an initial step for a rigorous stability analysis of a more general social potential fields model. Another similar work to ours is the work in [30]. However, there the work is limited to two dimensions and the stability analysis is very limited. Another related article using potential functions similar to ours is [35] and [36]. However, in [35] the model does not incorporate environmental effects and in [36] mostly quadratic gradient fields are considered. The results in this article were initially published in [54] and [55].

II. Swarm Model

We consider a swarm of M individuals (members) in an n-dimensional Euclidean space. We model the individuals as points and ignore their dimensions. The position of individual i is described by $x^i \in \mathbb{R}^n$. We assume synchronous motion and no time delays, i.e., all the individuals move simultaneously and know the exact relative position of all the other individuals. Let $\sigma : \mathbb{R}^n \to \mathbb{R}$ represent the attractant/repellent profile or the "σ-profile" which can be a profile of nutrients or some attractant or repellent substances (e.g., food/nutrients, pheromones laid by other individual, or toxic chemicals). Assume that the areas that are minimum points are "favorable" to the individuals in the swarm. For example, assume that $\sigma(y) < 0$ represents attractant or nutrient rich, $\sigma(y) = 0$ represents a neutral, and $\sigma(y) > 0$ represents a noxious environment at y. (Note that $\sigma(\cdot)$ can be a combination of several attractant or repellent profiles.)

We consider the equation of motion of each individual i described by

$$\dot{x}^i = -\nabla_{x^i}\sigma(x^i) + \sum_{j=1, j\neq i}^{M} g(x^i - x^j), i = 1, \ldots, M \quad (1)$$

where $g(\cdot)$ represents the function of mutual attraction and repulsion between the individuals and is an *odd* function of the form [51]

$$g(y) = -y\left[g_a\left(||y||\right) - g_r\left(||y||\right)\right] \quad (2)$$

where $g_a : \mathbb{R}^+ \to \mathbb{R}^+$ represents (the magnitude of) the attraction term and it has a *long range*, whereas $g_r : \mathbb{R}^+ \to \mathbb{R}^+$ represents (the magnitude of) the repulsion term and it has a *short range*, and $\|\cdot\|$ is the Euclidean norm. As in [51] it is assumed that $yg_a(||y||) = \nabla_y J_a(||y||)$ and $yg_r(||y||) = \nabla_y J_r(||y||)$, where $J_a(\cdot)$ and $J_r(\cdot)$ are the *artificial social potential functions* of the attraction and repulsion between the individuals, respectively. The functions $g_a(\cdot)$ and $g_r(\cdot)$ are chosen such that on large distances attraction dominates, on short distances repulsion dominates, and there is a unique constant distance δ where attraction and repulsion balance. In other words, we assume that there exists δ such that $g_a(\delta) = g_r(\delta)$, and for $||y|| > \delta$ we have $g_a(||y||) > g_r(||y||)$ and for $||y|| < \delta$ we have $g_r(||y||) > g_a(||y||)$. This is consistent with biological observations [3], [4], where the inter-individual attraction/repulsion is based on an interplay between attraction and repulsion forces with the attraction dominating on large distances, and the repulsion dominating on short distances. The distance δ, on which the attraction and repulsion between two individuals balance is called the *equilibrium distance* in the biological literature. However, we will not use this term here in order to avoid any confusion with the terminology in stability theory.

The term $-\nabla_{x^i}\sigma(x^i)$ represents the motion of the individuals toward regions with higher nutrient concentration and away from regions with high concentration of toxic substances. Note that the implicit assumption that the individuals know the gradient of the profile at their position is not very restrictive since it is known that some organisms such as bacteria are able to construct local approximations to gradients [23].

We would like to emphasize that even though we get our inspiration from biological swarms, our model constitutes also essentially a kinematic model for swarms of engineering multi-agent systems. In the context of multi-agent (i.e., multi-robot)

systems the profile $\sigma(\cdot)$ constitutes an *artificial potential function* that models the environment containing obstacles or threats to be avoided (analogous to toxic substances) and targets to be moved toward (analogous to food). In systems with real agents (with their specific dynamics) the trajectories generated by our model can be used as reference trajectories for the agents to follow or track.

Note also that, even though our model is a type of a kinematic model, it can be viewed as an approximation of a model with point mass swarm member dynamics for some organisms such as bacteria. To see this consider the point mass model in which the individuals move based on the Newton's law $m_i a^i = F^i$. This gives rise to the system of motion equations

$$\dot{x}^i = v^i$$
$$m_i \dot{v}^i = u^i$$

where $u^i = F^i$ is the total force acting on individual i. Now, suppose there is a velocity damping term of the form $-k_v v^i$ in u^i, where $k_v > 0$. In other words, assume that we have

$$u^i = -k_v v^i + \bar{u}^i.$$

Now, note that for organisms such as bacteria we have m_i very small (i.e., we have $m_i \approx 0$) and the viscosity of the environment for them is high. For this reason, we can take $m_i = 0$. Substituting this in the above system of equations we obtain

$$\dot{x}^i = \frac{1}{k_v}\bar{u}^i$$

which is exactly the same model that we consider in this article with $k_v = 1$ and

$$\bar{u}^i = -\nabla_{x^i}\sigma(x^i) - \sum_{j=1, j\neq i}^{M} \left[\nabla_{x^i} J_a\left(\|x^i - x^j\|\right) - \nabla_{x^i} J_r\left(\|x^i - x^j\|\right)\right].$$

Note that the above controller $\bar{u}^i$ is an *energy minimization* controller of the form

$$\bar{u}^i = -\nabla_{x^i} E,$$

where E is the *total artificial potential energy* in the system and is given by

$$E = \sum_{i=1}^{M}\sigma(x^i) + \frac{1}{2}\sum_{i=1}^{M}\sum_{j=1, j\neq i}^{M}\left[J_a\left(\|x^i - x^j\|\right) - J_r\left(\|x^i - x^j\|\right)\right].$$

Therefore, each of the individuals in the swarm moves such that to minimize the total artificial potential energy in the system.

One drawback of the model here is that each individual needs to know the *relative* position of *all* the other individuals. In biological swarms, often each individual can see (or sense) only the individuals in its neighborhood because the ranges of their senses are limited. Therefore, in nature the attraction or "desire to stick together" depends only on the individuals that it can sense. Therefore, the final behavior of the swarms described here may not be in "perfect harmony" with real biological swarms. For example, in real swarms we may observe formation of several separate clusters or swarms instead of a single swarm (as would be the case here). Moreover, in real swarms if the swarm arrives in the vicinity of two close valleys then swarm splitting may occur, whereas here it may not necessarily do so. Nevertheless, the analysis here is a first step toward developing a comprehensive and rigorous stability theory for social foraging of swarms. Moreover, in engineering applications the sensing limitations of the agents can be overcome with technologies such as global positioning system (GPS). Note also that with restrictions on the initial relative positions of the swarm members it may be possible to obtain local stability results for swarms in which the individuals have limited sensing (and therefore attraction) range. However, this will not be considered here. One can think of our swarm as a (predefined) team (or a set) of agents (robots) which know each others relative position and are required to gather around targets and avoid obstacles or threats.

The objective here is to analyze the qualitative properties of the collective behavior (motions in n-space) of the individuals. To this end we define the *center* of the swarm as $\bar{x} = 1/M\sum_{i=1}^{M} x^i$. Then, the motion of the center is given by

$$\dot{\bar{x}} = -\frac{1}{M}\sum_{i=1}^{M}\nabla_{x^i}\sigma(x^i) - \frac{1}{M}\sum_{i=1}^{M}\sum_{j=1, j\neq i}^{M} g(x^i - x^j) = -\frac{1}{M}\sum_{i=1}^{M}\nabla_{x^i}\sigma(x^i) \quad (3)$$

since we have

$$\frac{1}{M}\sum_{i=1}^{M}\sum_{j=1, j\neq i}^{M} g(x^i - x^j) = 0$$

which follows from the fact that $g(\cdot)$ are odd functions of the form of (2) and $g(x^i - x^j) = -g(x^j - x^i)$ for all pairs (i, j). The above equation implies that the center of the swarm moves along the *average* of the gradient of the profile evaluated at the current positions of the individuals. However, this does not necessarily mean that it will converge to a minimum. Moreover, this does not imply anything about the motions of the individuals. In fact, the convergence properties of the swarm to minimum (or critical) points of the profile depends on the properties of the profile.

One issue to note here is that as in [23] it is possible to view the foraging (and therefore social foraging) problem here as a *distributed optimization problem* (in which each individual is individually searching for the minimum) or optimal control problem, where the objective is to find the "optimal" control policy or search strategy that will maximize, for instance, the energy intake per time spent foraging. Here, we are not concerned with this problem. We specify the search strategy, which is a distributed gradient search, and are concerned with stability or convergence properties of the strategy. Still, however, it is an optimization or distributed function minimization problem and therefore, our results here have some relevance to the optimization literature. Note that in nature there are many species with a variety of foraging or search strategies; some of the previous are most certainly not gradient-based and hence lie outside the scope of this work.

Note that the collective behavior in (3) has a kind of averaging (filtering or smoothing) effect. This may be important if

the σ-profile is a noisy function (or there is a measurement error or noise in the system as discussed in [1], [2]). In other words, if the σ-profile were a "noisy function" and the individuals were moving individually (without inter-individual attraction/repulsion), then they could get stuck at a local minima, whereas if they swarm, since they are moving collectively, the other individuals will "pull" them out of such local minima. This in turn will lead to the fact that the individuals will perform better collectively (i.e., due to swarming) as seen in some biological examples [1], [2].

In this article we will consider attraction/repulsion functions which are continuous and have *linear attraction*, i.e., $g_a(\|x^i - x^j\|) = a$ for some $a > 0$ and all $\|x^i - x^j\|$, and *bounded repulsion*, i.e., $g_r(\|x^i - x^j\|)\|x^i - x^j\| \leq b$ for some $b > 0$ and all $\|x^i - x^j\|$. The continuity assumption is needed in order to guarantee the existence and uniqueness of the solutions of the system. This assumption leads to the fact that $g(\cdot)$ vanishes at the origin and brings a concern about collisions between the individuals. However, by setting the magnitude of the repulsion high enough it is possible to avoid collisions at the expense of getting a larger swarm size. Another possibility is to choose $g_r(\cdot)$ such that $g_r(\|x^i - x^j\|)\|x^i - x^j\| \to \infty$ as $\|x^i - x^j\| \to 0$ as will be discussed later. One function that satisfies the previous conditions is [49]

$$g(y) = -y\left[a - b\exp\left(-\frac{\|y\|^2}{c}\right)\right].$$

In the following sections, we will first perform cohesion analysis for the swarm under conditions satisfied by several profiles following which we will analyze the behavior of the swarm for several different profiles.

III. Cohesion Analysis

Before proceeding with analysis of the swarm behavior for different profiles in this section we will analyze the cohesiveness of the swarm under some general conditions satisfied by several profiles. To this end, we define the distance between the position x^i of individual i and the center $\bar{x}$ of the swarm as $e^i = x^i - \bar{x}$. The ultimate bound on the magnitude of e^i will quantify the size of the swarm. Note that

$$\dot{e}^i = -\nabla_{x^i}\sigma(x^i) - \sum_{j=1, j\neq i}^{M}\left[a - g_r\left(\|x^i - x^j\|\right)\right](x^i - x^j) + \frac{1}{M}\sum_{j=1}^{M}\nabla_{x^j}\sigma(x^j)$$

where $g_r(\cdot)$ is such that the boundedness assumption is satisfied. Defining a Lyapunov function as $V_i = (1/2)\|e^i\|^2 = (1/2)e^{i\top}e^i$, and since $e^i = (1/M)\sum_{j=1}^{M}(x^i - x^j)$ we obtain

$$\dot{V}_i = -aM\|e^i\|^2 + \sum_{j=1, j\neq i}^{M} g_r\left(\|x^i - x^j\|\right)(x^i - x^j)^\top e^i - \left[\nabla_{x^i}\sigma(x^i) - \frac{1}{M}\sum_{j=1}^{M}\nabla_{x^j}\sigma(x^j)\right]^\top e^i. \quad (4)$$

Now, if we can show that there is a constant ε such that for all $\|e^i\| > \varepsilon$ we have $\dot{V}_i < 0$, then we will guarantee that in that region $\|e^i\|$ is decreasing and eventually $\|e^i\| \leq \varepsilon$ will be achieved. With this in mind we have two assumptions about the profile. Note that these two assumptions do not have to be satisfied simultaneously.

Assumption 1: There exists a constant $\bar{\sigma} > 0$ such that

$$\|\nabla_y\sigma(y)\| \leq \bar{\sigma}$$

for all y.

Assumption 2: There exists a constant $A_\sigma > -aM$ such that

$$\left[\nabla_{x^i}\sigma(x^i) - \frac{1}{M}\sum_{j=1}^{M}\nabla_{x^j}\sigma(x^j)\right]^\top e^i \geq A_\sigma\|e^i\|^2$$

for all x^i and x^j.

Note that Assumption 1 requires only that the gradient of the profile to be bounded and is a very reasonable assumption that is satisfied with almost any realistic profile (e.g., plane and Gaussian profiles). In contrast, Assumption 2 is a more restrictive assumption. It requires the gradient of the profile at x^i to have a "large enough" component along e^i so that the effect of the profile does not prevent swarm cohesion. Therefore, it may be satisfied only by few profiles (e.g., a quadratic profile). With this in mind we state the following result.

Lemma 1: Consider the swarm described by the model in (1) with $g(\cdot)$ as given in (2) with linear attraction (i.e., $g_a(\|x^i - x^j\|) = a$ for some $a > 0$ and all $\|x^i - x^j\|$) and bounded repulsion, (i.e., $g_r(\|x^i - x^j\|)\|x^i - x^j\| \leq b$ for some $b > 0$ and all $\|x^i - x^j\|$). Then, as $t \to \infty$ we have $x^i(t) \to B_\varepsilon(\bar{x}(t))$, where

$$B_\varepsilon(\bar{x}(t)) = \{y(t) : \|y(t) - \bar{x}(t)\| \leq \varepsilon\}$$

and

- if Assumption 1 is satisfied, then
$$\varepsilon = \varepsilon_1 = \frac{(M-1)}{aM}\left[b + \frac{2\bar{\sigma}}{M}\right];$$
- if Assumption 2 is satisfied, then
$$\varepsilon = \varepsilon_2 = \frac{b(M-1)}{aM + A_\sigma}.$$

Proof:

Case 1) From the $\dot{V}_i$ equation we obtain

$$\dot{V}_i \leq -aM\|e^i\|^2 + \sum_{j=1, j\neq i}^{M} g_r\left(\|x^i - x^j\|\right)\|x^i - x^j\|\|e^i\| + \left\|\nabla_{x^i}\sigma(x^i) - \frac{1}{M}\sum_{j=1}^{M}\nabla_{x^j}\sigma(x^j)\right\|\|e^i\| \leq -aM\|e^i\|\left[\|e^i\| - \frac{b(M-1)}{aM} - \frac{2\bar{\sigma}(M-1)}{aM^2}\right]$$

which implies that as long as $\|e^i\| > \varepsilon_1$ we have $\dot{V}_i < 0$. Above to obtain the last inequality we used

the fact that $g_r(\|x^i - x^j\|)\|x^i - x^j\| \leq b$ and the inequality

$$\left\| \nabla_{x^i}\sigma(x^i) - \frac{1}{M}\sum_{j=1}^{M} \nabla_{x^j}\sigma(x^j) \right\| \leq \frac{2\bar{\sigma}(M-1)}{M}$$

which follows from Assumption 1.

Case 2) Similarly using Assumption 2 one can show that $\dot{V}_i$ satisfies

$$\dot{V}_i \leq -(aM + A_\sigma)\|e^i\| \left[\|e^i\| - \frac{b(M-1)}{aM + A_\sigma} \right].$$

Therefore, we conclude that as long as $\|e^i\| > \varepsilon_2$ we have $\dot{V}_i < 0$. ■

This result is important because it proves the cohesiveness of the swarm and provides a bound on the swarm size, defined as the radius of the hyperball centered at $\bar{x}(t)$ and containing all the individuals. Therefore, in order to analyze the collective behavior of the swarm we need to consider the motion of the center.

In species that engage in social foraging it has been observed that the individuals in swarms desire to be close (but not too close) to other individuals. In the mean time, they want to find more food. The balance between these desires determines the size of the swarm (herd, flock or school). Our model captures this by having an inter-individual attraction/repulsion term and also a term due to the environment (or the nutrient profile) affecting their motion. In the results above, the resulting swarm sizes depend on the inter-individual attraction/repulsion parameters (a and b) and the parameters of the nutrient profile ($\bar{\sigma}$ and A_σ). Moreover, the dependence on these parameters makes intuitive sense. Larger attraction (larger a) leads to a smaller swarm size, larger repulsion (larger b) leads to a larger swarm size, larger $\bar{\sigma}$ (fast changing landscape) leads to a larger swarm. These concepts are present in foraging theory in biology and model the balance of the desire of the individuals to "stick together" with the desire to "get more food" that was created by evolutionary forces. Note that for Assumption 2 to be satisfied we have the condition $A_\sigma > -aM$. The threshold $A_\sigma = -aM$ is the point at which the inter-individual attraction is not anymore guaranteed to "hold the swarm together" since it might be counterbalanced by the repulsion from the profile. In other words, beyond that threshold the repulsion from the center of the profile (i.e., toxic substances) is so intense that the "desire to keep away from the center of the profile" may dominate (or be more plausible than) the "desire to stick together." Therefore, if this condition is not satisfied we cannot anymore guarantee cohesiveness of the swarm, i.e., it can happen that the swarm members move arbitrary far from each other. This helps to quantify the inherent balance between the sometimes conflicting desires for swarm cohesiveness and for following cues from the environment to find food. Such behavior can be seen in, for example, fish schools when a predator attacks the school. In that case the fish move very fast in all directions away from the predator [56].

Note that the desire of the individuals to "stick together" depends on the inter-individual attraction parameter a and the number of individuals M. This is consistent with *some* biological swarms, where it has been observed that individuals are attracted more to larger (or more crowded) swarms (even though that attraction may not be linearly proportional to the number of individuals). In nature the values of the parameters governing the swarm motion have been tuned for millions of years by the evolutionary process.

One issue to note here is that as M gets large both ε_1 and ε_2 approach constant values. This implies that for a large M the individuals will form a cohesive swarm of a constant size independent of the number of the individuals and the characteristics of the profile. Unfortunately, this is not biologically very realistic.

The above result is an asymptotic result, i.e., $x^i(t) \to B_\varepsilon(\bar{x}(t))$ as $t \to \infty$. However, from stability theory we know that for any $\varepsilon^* > \varepsilon$, $x^i(t)$ will enter $B_{\varepsilon^*}(\bar{x}(t))$ in a finite time. In other words, it can be shown that the swarm of any size a little larger than ε will be formed in a finite time.

In the following sections, we will analyze the behavior of the swarm on different profiles. In particular, we will consider plane, quadratic, Gaussian, and multimodal Gaussian profiles.

IV. Motion Along a Plane Attractant/Repellent Profile

In this section we assume that the profile is described by a *plane* equation of the form

$$\sigma(y) = a_\sigma^\top y + b_\sigma \tag{5}$$

where $a_\sigma \in \mathbb{R}^n$ and $b_\sigma \in \mathbb{R}$. One can see that the gradient of the profile is given by

$$\nabla_y \sigma(y) = a_\sigma$$

and Assumption 1 holds with $\bar{\sigma} = \|a_\sigma\|$. However, note also that

$$\nabla_{x^i}\sigma(x^i) - \frac{1}{M}\sum_{j=1}^{M} \nabla_{x^j}\sigma(x^j) = 0$$

for all i, implying that the last term in (4) vanishes. Therefore, for this profile the bound on the swarm size is given by

$$\varepsilon = \varepsilon_p = \frac{b(M-1)}{aM} < \frac{b}{a}.$$

Note also that for this case we have

$$\dot{\bar{x}}(t) = -a_\sigma$$

which implies that the center of the swarm will be moving with the constant velocity vector $-a_\sigma$ (and eventually will diverge toward infinity where the minimum of the profile occurs).

The motions in this section can be viewed as a model of a foraging herd that moves in a constant direction (while keeping its cohesiveness) with a constant speed such as the one considered in [57]. Another view of the system in this section could be as a model of a multi-agent system in which the autonomous agents move in a formation with a constant speed. In fact, transforming the system to e^i coordinates we obtain

$$\dot{e}^i = \sum_{j=1, j\neq i}^{M} g(e^i - e^j), i = 1, \ldots, M$$

which is exactly the model of an aggregating swarm considered in [49]. Therefore, all the results obtained in [49] apply for e^i. In particular, we have $\dot{e}^i(t) \to 0$ as $t \to \infty$. In other words, the swarm converges to a constant configuration or a formation (i.e., constant relative positions) that moves with a constant speed in the direction of $-a_\sigma$. The only drawback is that for the given swarm model we cannot a priori specify the formation to be established. However, note that it is possible to modify the swarm model such that the inter-individual attraction/repulsion functions $g(\cdot)$ is pair dependent, i.e., there is a different $g_{i,j}(\cdot)$ for a different pair (i,j). Then, by appropriate choice of each $g_{i,j}(\cdot)$ one can achieve any desired formation.

V. Quadratic Attractant/Repellent Profiles

In this section, we will consider a *quadratic* profile given by

$$\sigma(y) = \frac{A_\sigma}{2}\|y - c_\sigma\|^2 + b_\sigma \tag{6}$$

where $A_\sigma \in \mathbb{R}$, $b_\sigma \in \mathbb{R}$, and $c_\sigma \in \mathbb{R}^n$. Note that this profile has a global extremum (either a minimum or a maximum depending on the sign of A_σ) at $y = c_\sigma$. Its gradient at a point $y \in \mathbb{R}^n$ is given by

$$\nabla_y \sigma(y) = A_\sigma(y - c_\sigma).$$

Assume that $A_\sigma > -aM$. Then, with few manipulations one can show that for this profile Assumption 2 holds with strict equality. Therefore, the result of Lemma 1 holds with the bound

$$\varepsilon_q = \varepsilon_2 = \frac{b(M-1)}{aM + A_\sigma}.$$

Now, let us analyze the motion of the center $\bar{x}$. Substituting the gradient in the equation of motion of $\bar{x}$ given in (3) we obtain

$$\dot{\bar{x}} = -A_\sigma(\bar{x} - c_\sigma).$$

Defining the distance between the center $\bar{x}$ and the extremum point c_σ as $e_\sigma = \bar{x} - c_\sigma$, we have

$$\dot{e}_\sigma = -A_\sigma e_\sigma$$

which implies that as $t \to \infty$ we have $e_\sigma(t) \to 0$ if $A_\sigma > 0$ and that $e_\sigma(t) \to \infty$ if $A_\sigma < 0$ and $e_\sigma(0) \neq 0$. Therefore, we have the following result.

Lemma 2: Consider the swarm described by the model in (1) with $g(\cdot)$ as given in (2). Assume that the σ-profile of the environment is given by (6). As $t \to \infty$ we have

- if $A_\sigma > 0$, then $\bar{x}(t) \to c_\sigma$ (i.e., the center of the swarm converges to the global minimum c_σ of the profile);
- if $A_\sigma < 0$ and $\bar{x}(0) \neq c_\sigma$, then $\bar{x}(t) \to \infty$ (i.e., the center of the swarm diverges from the global maximum c_σ of the profile).

Note that this result holds for any A_σ (i.e., we do not need the assumption $A_\sigma > -aM$). Note also that for the case with $A_\sigma > 0$ for any finite $\varepsilon^* > 0$ (no matter how small) it can be shown that $\|\bar{x}(t) - c_\sigma\| < \varepsilon^*$ is satisfied in a finite time. In other words, $\|\bar{x}\|$ enters any ε^* neighborhood of c_σ in a finite time. In contrast, for the case with $A_\sigma < 0$ and $\bar{x}(0) \neq c_\sigma$ for any $D > 0$ (no matter how large) it can be shown that $\|\bar{x}(t) - c_\sigma\| > D$ is satisfied in a finite time, implying that $\|\bar{x}\|$ exits any bounded D-neighborhood of c_σ in a finite time. If $A_\sigma < 0$ and $\bar{x}(0) = c_\sigma$, on the other hand, then $\bar{x}(t) = c_\sigma$ for all t. In other words, for this case the swarm will be either "trapped" around the maximum point because of the inter-individual attraction (i.e., desire of the individuals to be close to each other) or will disperse in all directions if the inter-individual attraction is not strong enough (i.e., $A_\sigma < -aM$). Note, however, that even if they disperse, the center $\bar{x}$ will not move and stay at c_σ. Such a dispersal behavior can be seen in fish schools when attacked by a predator [56]. In other words, for the fish the effect of the presence of a predator can be modeled by a large intensity repellent profile.

Here, we did not consider the $A_\sigma = 0$ case. This is because if $A_\sigma = 0$ then the profile is uniform everywhere and $\nabla_y \sigma(y) = 0$ for all $y \in \mathbb{R}^n$. Therefore, the existence of the profile does not affect the motion of the individuals and stability analysis is reduced to the one described in [49], where nondrifting aggregating swarms were considered and it was shown that the swarm will cluster around the stationary center $\bar{x}$.

Combining the results of Lemmas 1 and 2 together with the above observations gives us the following result.

Theorem 1: Consider the swarm described by the model in (1) with inter-individual attraction/repulsion function $g(\cdot)$ as given in (2) with linear attraction and bounded repulsion. Assume that the σ-profile of the environment is given by (6) and that $A_\sigma > -aM$. Then, the following hold

- if $A_\sigma > 0$, then for any $\varepsilon^* > \varepsilon_q$ all individuals $i = 1, \ldots, M$, will enter $B_{\varepsilon^*}(c_\sigma)$ in a finite time;
- if $A_\sigma < 0$ and $\bar{x}(0) \neq c_\sigma$, then for any $D < \infty$ all individuals $i = 1, \ldots, M$, will exit $B_D(c_\sigma)$ in a finite time.

This result is important because it gives finite time convergence (divergence) of *all* the individuals to nutrient rich (from toxic) regions of the profile.

Now, assume that instead of the profile in (6) we have a profile which is a sum of quadratic functions. In other words, assume that the profile is given by

$$\sigma(y) = \sum_{i=1}^{N} \frac{A_\sigma^i}{2}\|y - c_\sigma^i\|^2 + b_\sigma$$

where $A_\sigma^i \in \mathbb{R}$, and $c_\sigma^i \in \mathbb{R}^n$ for all $i = 1, \ldots, N$, and $b_\sigma \in \mathbb{R}$. Its gradient at a point y is given by

$$\nabla_y \sigma(y) = \sum_{i=1}^{N} A_\sigma^i \left(y - c_\sigma^i\right).$$

Defining

$$A_\sigma = \sum_{i=1}^{N} A_\sigma^i$$

and

$$c_\sigma = \frac{\sum_{i=1}^{N} A_\sigma^i c_\sigma^i}{\sum_{i=1}^{N} A_\sigma^i}$$

we obtain

$$\nabla_y \sigma(y) = A_\sigma(y - c_\sigma)$$

which is exactly the same as above. The point c_σ is the point of the unique extremum of the combined profile function. Therefore, the above results will directly transfer without any modification. This also is true because it can be shown that

$$\sum_{i=1}^{N} \frac{A_\sigma^i}{2} \left\|y - c_\sigma^i\right\|^2 = \frac{A_\sigma}{2}\|y - c_\sigma\|^2 + C$$

where C is a constant.

Quadratic profiles are rather simple profiles and the results in this section are intuitively expected. However, note also that more complicated profiles can be locally modeled (or approximated) as quadratic in regions near extremum points. In the following sections, we will consider profiles which are not necessarily quadratic or even convex. Moreover, later we will allow the profile to have multiple extremum points.

VI. Gaussian Attractant/Repellent Profiles

In this section, we consider profiles that are described by a Gaussian-type of equation

$$\sigma(y) = -\frac{A_\sigma}{2} \exp\left(-\frac{\|y - c_\sigma\|^2}{l_\sigma}\right) + b_\sigma \tag{7}$$

where $A_\sigma \in \mathbb{R}$, $b_\sigma \in \mathbb{R}$, $l_\sigma \in \mathbb{R}^+$, and $c_\sigma \in \mathbb{R}^n$. Note that this profile also has the unique extremum (either a global minimum or a global maximum depending on the sign of A_σ) at $y = c_\sigma$. Its gradient is given by

$$\nabla_y \sigma(y) = \frac{A_\sigma}{l_\sigma}(y - c_\sigma) \exp\left(-\frac{\|y - c_\sigma\|^2}{l_\sigma}\right).$$

Calculating the time derivative of the center of the swarm by using (3) one can obtain

$$\dot{\bar{x}} = -\frac{A_\sigma}{Ml_\sigma} \sum_{i=1}^{M} (x^i - c_\sigma) \exp\left(-\frac{\|x^i - c_\sigma\|^2}{l_\sigma}\right).$$

Compared to the quadratic case, here we cannot write $\dot{\bar{x}}$ as a function of $e_\sigma = \bar{x} - c_\sigma$. This is basically because of the nonlinearity of the gradient of the profile. However, intuitively we would expect that we still should be able to get some results similar to the ones in the preceding section. To this end we note that Assumption 1 is satisfied with

$$\bar{\sigma} = \frac{|A_\sigma|}{\sqrt{2}l_\sigma} \exp\left(-\frac{1}{2}\right).$$

Therefore, Lemma 1 holds and we know that as $t \to \infty$ all the individuals will converge to (and stay within) the

$$\varepsilon_G = \varepsilon_1 = \frac{(M-1)}{aM}\left[b + \frac{|A_\sigma|}{M}\sqrt{\frac{2}{l_\sigma}} \exp\left(-\frac{1}{2}\right)\right]$$

neighborhood of the (mobile) center $\bar{x}$.

Now, we have to analyze the motion of $\bar{x}$ in order to determine the overall behavior of the swarm.

Lemma 3: Consider the swarm described by the model in (1) with inter-individual attraction/repulsion function $g(\cdot)$ as given in (2). Assume that the σ-profile of the environment is given by (7). Then, as $t \to \infty$ we have

- if $A_\sigma > 0$, then $\|e_\sigma(t)\| \leq \max_{i=1,\ldots,M} \|e^i(t)\| \triangleq e_{max}(t)$;
- if $A_\sigma < 0$ and $\|e_\sigma(0)\| > e_{max}(0)$ (here we assume that $x^i(0) \neq x^j(0)$ for all pairs of individuals $(i, j), j \neq i, 1 \leq i, j \leq M$ and therefore $e_{max}(0) > 0$), then $\|e_\sigma\| \to \infty$.

Proof: To start with, let $V_\sigma = (1/2)e_\sigma^\top e_\sigma$. Then, its derivative along the motion of the swarm is given by

$$\begin{aligned}\dot{V}_\sigma &= -\frac{A_\sigma}{Ml_\sigma} \sum_{i=1}^{M} \exp\left(-\frac{\|x^i - c_\sigma\|^2}{l_\sigma}\right)(x^i - c_\sigma)^\top e_\sigma \\ &= -\frac{A_\sigma}{Ml_\sigma} \sum_{i=1}^{M} \exp\left(-\frac{\|x^i - c_\sigma\|^2}{l_\sigma}\right)\|e_\sigma\|^2 \\ &\quad -\frac{A_\sigma}{Ml_\sigma} \sum_{i=1}^{M} \exp\left(-\frac{\|x^i - c_\sigma\|^2}{l_\sigma}\right) e^{i\top} e_\sigma\end{aligned}$$

where we used the fact that $x^i - c_\sigma = e^i + e_\sigma$.

a) *Case 1*: $A_\sigma > 0$:: Bounding $\dot{V}_\sigma$ from above we obtain

$$\begin{aligned}\dot{V}_\sigma &\leq -\frac{A_\sigma}{Ml_\sigma} \sum_{i=1}^{M} \exp\left(-\frac{\|x^i - c_\sigma\|^2}{l_\sigma}\right)\|e_\sigma\|^2 \\ &\quad + \frac{A_\sigma}{Ml_\sigma} \sum_{i=1}^{M} \exp\left(-\frac{\|x^i - c_\sigma\|^2}{l_\sigma}\right)\|e^i\|\|e_\sigma\| \\ &\leq -\frac{A_\sigma}{Ml_\sigma} \sum_{i=1}^{M} \exp\left(-\frac{\|x^i - c_\sigma\|^2}{l_\sigma}\right)\|e_\sigma\| \\ &\quad \times \left[\|e_\sigma\| - \frac{\sum_{i=1}^{M} \exp\left(-\frac{\|x^i - c_\sigma\|^2}{l_\sigma}\right)\|e^i\|}{\sum_{i=1}^{M} \exp\left(-\frac{\|x^i - c_\sigma\|^2}{l_\sigma}\right)}\right] \\ &\leq -\frac{A_\sigma}{Ml_\sigma} \sum_{i=1}^{M} \exp\left(-\frac{\|x^i - c_\sigma\|^2}{l_\sigma}\right)\|e_\sigma\|\left[\|e_\sigma\| - e_{max}\right]\end{aligned}$$

where $e_{max} = \max_{i=1,\ldots,M} \|e^i\|$. The above inequality implies that as long as $\|e_\sigma(t)\| > e_{max}(t)$, i.e., the minimum point c_σ is outside the swarm boundary, then the center of the swarm will be moving toward it. Therefore, as $t \to \infty$ we will asymptotically have $\|e_\sigma(t)\| \leq e_{max}(t)$, i.e., c_σ will be within the swarm.

b) *Case 2*: $A_\sigma < 0$:: With analysis similar to the case 1 above it can be shown that

$$\dot{V}_\sigma \geq \frac{|A_\sigma|}{Ml_\sigma} \sum_{i=1}^{M} \exp\left(-\frac{\|x^i - c_\sigma\|^2}{l_\sigma}\right)\|e_\sigma\|\left[\|e_\sigma\| - e_{max}\right]$$

which implies that we have $\dot{V}_\sigma > 0$. In other words, if $\|e_\sigma\| > e_{max}$, then $\|e_\sigma\|$ will increase. From Lemma 1 we have that e_{max} is decreasing. Therefore, since by hypothesis $\|e_\sigma(0)\| > e_{max}(0)$ we have that $\dot{V}_\sigma > 0$ holds. Now, given any large but fixed $D > 0$ and $\|e_\sigma(t)\| \leq D$ we have

$$\exp\left(-\frac{\|x^i - c_\sigma\|^2}{l_\sigma}\right)\|e_\sigma\|\left[\|e_\sigma\| - e_{max}\right] \geq \exp\left(-\frac{\left(D^2 + \varepsilon_3^2\right)}{l_\sigma}\right) D[D - \varepsilon_3] > 0$$

implying that

$$\dot{V}_\sigma \geq \frac{|A_\sigma|}{l_\sigma} \exp\left(-\frac{(D^2+\varepsilon_G^2)}{l_\sigma}\right) D[D-\varepsilon_G] > 0$$

from which using (a corollary to) the Chetaev Theorem [58] we conclude that $||e_\sigma||$ will exit the D-neighborhood of c_σ. ∎

Note that the result in Lemma 3 makes intuitive sense. If we have a hole (i.e., a minimum) it guarantees that the individuals will "gather" around it (as expected). If we have a hill (i.e., a maximum) and all the individuals are located on one side of the hill, it guarantees that the individuals diverge from it (as expected). If there is a hill, but the individuals are spread around it, then we cannot conclude neither convergence nor divergence. This is because it can happen that the swarm may move to one side and diverge or the inter-individual attraction forces can be counterbalanced by the inter-individual repulsion combined with the repulsion from the hill so that the swarm does not move away from the hill.

The above result (in Lemma 3) together with the result in Lemma 1 allow us to state the following.

Theorem 2: Consider the swarm described by the model in (1) with inter-individual attraction/repulsion function $g(\cdot)$ as given in (2) with linear attraction and bounded repulsion. Assume that the σ-profile of the environment is given by (7). Then, as $t \to \infty$ we have

- if $A_\sigma > 0$, then all individuals $i = 1, \ldots, M$, will enter (and stay within) $B_{2\varepsilon_G}(c_\sigma)$;
- if $A_\sigma < 0$ and $||e_\sigma(0)|| \geq e_{max}(0)$, then all individuals $i = 1, \ldots, M$, will exit $B_D(c_\sigma)$ for any fixed $D > 0$.

For the case $A_\sigma > 0$ Lemma 1 states that the swarm will have a maximum size of ε_G, i.e., $||e_\sigma|| \leq \varepsilon_G$ for all $i = 1, \ldots, M$, and Lemma 3 states that the swarm center will converge to the e_{max} and therefore to the ε_G neighborhood of c_σ, i.e., $||e_\sigma|| \leq e_{max} \leq \varepsilon_G$. Combining these two bounds we obtain the $2\varepsilon_G$ in the first case in Theorem 2.

Theorem 2 is a parallel of Theorem 1. However, here we have a weaker result since for the $A_\sigma > 0$ case we cannot guarantee that $\bar{x}(t) \to c_\sigma$. Moreover, the region around c_σ in which the individuals converge is larger ($2\varepsilon_G$) compared to the region in Theorem 1 (ε_q).

The drawback of this and the previous case is that both have a single extremum (which is either a minimum or a maximum) and the profile is relatively "uniform." In the next section, we will consider a profile for which this is not necessarily the case.

VII. Multimodal Gaussian Attractant/Repellent Profiles

Now, we will consider a profile which is a combination of *Gaussian* profiles. In other words, we will consider the profiles given by

$$\sigma(y) = -\sum_{i=1}^{N} \frac{A_\sigma^i}{2} \exp\left(-\frac{\left\|y - c_\sigma^i\right\|^2}{l_\sigma^i}\right) + b_\sigma \qquad (8)$$

where $c_\sigma^i \in \mathbb{R}^n$, $l_\sigma^i \in \mathbb{R}^+$, $A_\sigma^i \in \mathbb{R}$ for all $i = 1, \ldots, N$, and $b_\sigma \in \mathbb{R}$. Note that since the A_σ^i's can be positive or negative there can be both hills and valleys leading to a "more irregular" profile. In [23], where social foraging was considered as an optimization process, a profile of this type was considered and convergence to minima of the profile was shown in simulation.

The gradient of the profile at a point y is given by

$$\nabla_y \sigma(y) = \sum_{i=1}^{N} \frac{A_\sigma^i}{l_\sigma^i} \left(y - c_\sigma^i\right) \exp\left(-\frac{\left\|y - c_\sigma^i\right\|^2}{l_\sigma^i}\right).$$

Note that for this profile Assumption 1 is satisfied with

$$\bar{\sigma} = \sum_{i=1}^{N} \frac{\left|A_\sigma^i\right|}{\sqrt{2 l_\sigma^i}} \exp\left(-\frac{1}{2}\right).$$

Therefore, from Lemma 1 we have

$$\varepsilon_{mG} = \varepsilon_1 = \frac{(M-1)}{aM}\left[b + \frac{1}{M}\sum_{i=1}^{N}\left|A_\sigma^i\right|\sqrt{\frac{2}{l_\sigma^i}}\exp\left(-\frac{1}{2}\right)\right]$$

as the bound on the swarm size. In other words, as $t \to \infty$ we will have $x^i(t) \to B_{\varepsilon_{mG}}(\bar{x}(t))$, where ε_{mG} is as given above.

Using the profile gradient equation we can write the equation of motion of the swarm center $\bar{x}$ as

$$\dot{\bar{x}} = -\frac{1}{M}\sum_{j=1}^{N}\frac{A_\sigma^j}{l_\sigma^j}\sum_{i=1}^{M}\left(x^i - c_\sigma^j\right)\exp\left(-\frac{\left\|x^i - c_\sigma^j\right\|^2}{l_\sigma^j}\right).$$

As one can see, it is not obvious from this equation how the center $\bar{x}$ will move. Therefore, for this type of profile it is not easy to prove convergence of the individuals to a minimum of the profile for the general case. However, under some conditions it is possible to prove convergence to the vicinity of a particular c_σ^j (if c_σ^j is the center of a valley) or divergence from the neighborhood of a particular c_σ^j (if c_σ^j is the center of a hill).

Lemma 4: Consider the swarm described by the model in (1) with $g(\cdot)$ as given in (2). Assume that the σ-profile of the environment is given by (8). Moreover, assume that for some k, $1 \leq k \leq N$, we have

$$\left\|x^i(0) - c_\sigma^k\right\| \leq h_k\sqrt{l_\sigma^k}$$

for some h_k and for all $i = 1, \ldots, M$, and that for all $j = 1, \ldots, N$, $j \neq k$ we have

$$\left\|x^i(0) - c_\sigma^j\right\| \geq h_j\sqrt{l_\sigma^j}$$

for some h_j, $j = 1, \ldots, N$, $j \neq k$ and for all $i = 1, \ldots, M$. (This means that the swarm is near c_σ^k and far from other c_σ^j, $j \neq k$.) Moreover, assume that

$$\frac{A_\sigma^k}{\sqrt{l_\sigma^k}} h_k \exp\left(-h_k^2\right) > \frac{1}{\alpha}\sum_{j=1, j\neq k}^{N}\frac{\left|A_\sigma^j\right|}{\sqrt{l_\sigma^j}} h_j \exp\left(-h_j^2\right)$$

is satisfied for some $0 < \alpha < 1$. Then, for $e_\sigma^k = \bar{x} - c_\sigma^k$ as $t \to \infty$ we will have

- if $A_\sigma^k > 0$, then $||e_\sigma^k(t)|| \leq \varepsilon_{mG} + \alpha h_k\sqrt{l_\sigma^k}$;

- if $A_\sigma^k < 0$ and $\|e_\sigma^k(0)\| \geq e_{max}(0) + \alpha h_k\sqrt{l_\sigma^k}$, then $\|e_\sigma^k(t)\| \geq \varepsilon_{mG} + \alpha h_k\sqrt{l_\sigma^k}$, where $e_{max} = \max_{i=1,\ldots,M}\|e^i\|$.

Proof: Let $V_\sigma^k = (1/2)e_\sigma^{k\top}e_\sigma^k$ be the Lyapunov function.

Case 1) $A_\sigma^k > 0$: Taking the derivative of V_σ^k along the motion of the swarm one can show that

$$\dot{V}_\sigma^k \leq -\frac{A_\sigma^k}{Ml_\sigma^k}\sum_{i=1}^{M}\exp\left(-\frac{\left\|x^i - c_\sigma^k\right\|^2}{l_\sigma^k}\right)\left\|e_\sigma^k\right\| \times\left[\left\|e_\sigma^k\right\| - e_{max} - \alpha h_k\sqrt{l_\sigma^k}\right]$$

which implies that we have $\dot{V}_\sigma^k < 0$ as long as $\|e_\sigma^k\| > e_{max} + \alpha h_k\sqrt{l_\sigma^k}$, and from Lemma 1 we know that as $t \to \infty$ we have $e_{max}(t) \leq \varepsilon_{mG}$.

Case 2) $A_\sigma^k < 0$: Similar to above, for this case it can be shown that

$$\dot{V}_\sigma^k \geq \frac{\left|A_\sigma^k\right|}{Ml_\sigma^k}\sum_{i=1}^{M}\exp\left(-\frac{\left\|x^i - c_\sigma^k\right\|^2}{l_\sigma^k}\right)\left\|e_\sigma^k\right\| \times\left[\left\|e_\sigma^k\right\| - e_{max} - \alpha h_k\sqrt{l_\sigma^k}\right]$$

which implies that if $\|e_\sigma^k\| > e_{max} + \alpha h_k\sqrt{l_\sigma^k}$, then we have $\dot{V}_\sigma > 0$. In other words, $\|e_\sigma^k\|$ will increase. From Lemma 1 we have that e_{max} is decreasing. Therefore, since by hypothesis $\|e_\sigma^k(0)\| > e_{max}(0) + \alpha h_k\sqrt{l_\sigma^k}$ we have that $\dot{V}_\sigma > 0$ holds at $t = 0$. Now, consider the boundary $\|e_\sigma^k\| = \varepsilon_{mG} + h_k\sqrt{l_\sigma^k}$. It can be shown that on the boundary we have

$$\dot{V}_\sigma \geq \frac{\left|A_\sigma^k\right| h_k(1-\alpha)\left(\varepsilon_{mG} + h_k\sqrt{l_\sigma^k}\right)\exp\left(-h_k^2\right)}{\sqrt{l_\sigma^k}} > 0$$

from which once again using (a corollary to) the Chetaev Theorem we conclude that $\|e_\sigma^k\|$ will exit the $\varepsilon_{mG} + h_k\sqrt{l_\sigma^k}$-neighborhood of c_σ^k. ■

Now, as in the preceding section we can combine this result (i.e., Lemma 4) together with Lemma 1 to obtain the following theorem.

Theorem 3: Consider the swarm described by the model in (1) with inter-individual attraction/repulsion function $g(\cdot)$ as given in (2) with linear attraction and bounded repulsion. Assume that the σ-profile of the environment is given by (8). Assume that the conditions of Lemma 4 hold. Then, as $t \to \infty$ all individuals will

- enter the hyperball $B_{\varepsilon_5}(c_\sigma^k)$, where $\varepsilon_5 = 2\varepsilon_{mG} + \alpha h_k\sqrt{l_\sigma^k}$, if $A_\sigma^k > 0$;
- leave the $h_k\sqrt{l_\sigma^k}$-neighborhood of c_σ^k, if $A_\sigma^k < 0$.

The only drawback of the above result is that we need

$$2\varepsilon_{mG} + \alpha h_k\sqrt{l_\sigma^k} < h_k\sqrt{l_\sigma^k}$$

in order for the result to make sense. This implies that we need

$$\varepsilon_{mG} < \left(\frac{1-\alpha}{2}\right)h_k\sqrt{l_\sigma^k}$$

which sometimes may not be easy to satisfy. However, one issue to note is that ε_{mG} is a very conservative bound. In reality, the actual size of the swarm is typically much smaller than the bound. Therefore, effectively, ε_{mG} can be replaced with $e_{max}(\infty) < \varepsilon_{mG}$ and it may be easier to satisfy the above condition.

VIII. Tighter Bounds, Unbounded Repulsion, and Collision Avoidance

The bounds on the swarm size obtained in Lemma 1 are rather conservative. In this section, we will show that for at least some of the cases it is possible to obtain a tighter bound on the *root-mean-square* of the distances of the individuals to their center. Moreover, we will allow for unbounded repulsion functions which could be used to guarantee collision avoidance or, in other words, will prevent two individuals to occupy the same space (an issue that was overlooked before).

The repulsion functions that we consider are assumed to satisfy [51]

i) as $\|x^i - x^j\| \to 0$, we have $g_r(\|x^i - x^j\|)\|x^i - x^j\| \to \infty$ (hence unbounded repulsion);

ii) $g_r(\|x^i - x^j\|) \leq (b)/(\|x^i - x^j\|^2)$, for some $b > 0$.

Note that provided that $x^i(0) \neq x^j(0)$ for all pairs (i,j), $j \neq i$, condition *i)* above will guarantee that $x^i(t) \neq x^j(t)$ for all pairs (i,j), $j \neq i$ and for all $t \geq 0$. Condition *ii)*, on the other hand, brings some restrictions on the growth of the repulsion and will be useful in the Lyapunov analysis.

Now, consider the Lyapunov function

$$V = \sum_{i=1}^{M} V_i + MV_\sigma$$

where V_i are the terms quantifying cohesion and are given by $V_i = (1/2)\|e^i\|^2$ and V_σ represents the distance to a minimum of the profile and is

- $V_\sigma = 0$ for a plane profile;
- $V_\sigma = 1/2\|e_\sigma\|^2$ for quadratic and Gaussian profiles;
- $V_\sigma = (1/2)\|e_\sigma^k\|^2$ for some $k, 1 \leq k \leq N$ for the multimodal Gaussian profile.

Taking the derivative of V we obtain

$$\begin{aligned}\dot{V} = &-aM\sum_{i=1}^{M}\|e^i\|^2 \\ &+\sum_{i=1}^{M}\sum_{j=1,j\neq i}^{M} g_r\left(\|x^i - x^j\|\right)(x^i - x^j)^\top e^i \\ &-\sum_{i=1}^{M}\left[\nabla_{x^i}\sigma(x^i) - \frac{1}{M}\sum_{j=1}^{M}\nabla_{x^j}\sigma(x^j)\right]^\top e^i \\ &-\sum_{i=1}^{M}\nabla_{x^i}\sigma^\top(x^i)e_\sigma.\end{aligned}$$

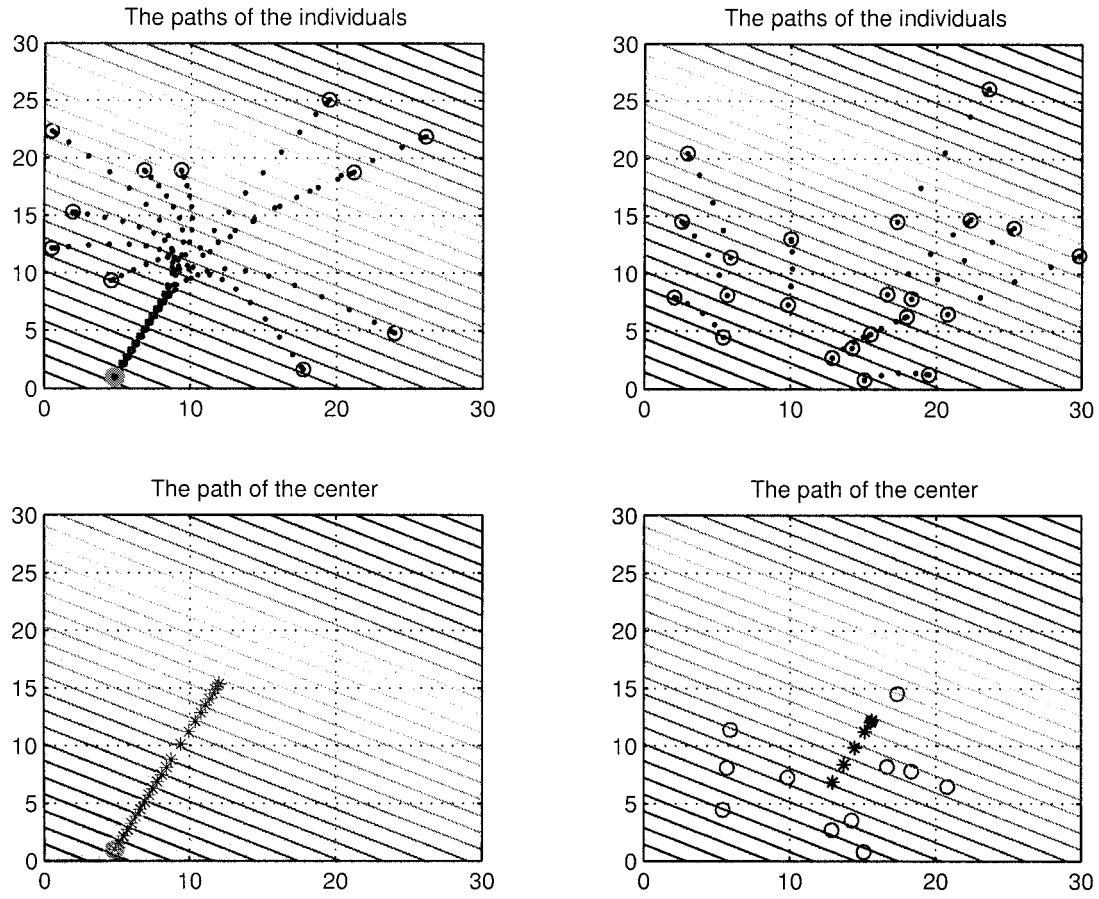

Fig. 1. Response for a plane profile.

Consider the third term on the right hand side (denoted with A below). With few manipulations it can be shown that we have

$$A = \sum_{i=1}^{M} \left[\nabla_{x^i}\sigma(x^i) - \frac{1}{M}\sum_{j=1}^{M} \nabla_{x^j}\sigma(x^j) \right]^{\top} e^i$$
$$= \sum_{i=1}^{M} \nabla_{x^i}\sigma^{\top}(x^i)(x^i - c_\sigma) - \sum_{i=1}^{M} \nabla_{x^i}\sigma^{\top}(x^i) e_\sigma.$$

Now, consider the second term on the right hand side of the above equation (denoted with B below). After some manipulations it can be shown that we have

$$B = \sum_{i=1}^{M}\sum_{j=1, j\neq i}^{M} g_r\left(\|x^i - x^j\|\right)(x^i - x^j)^{\top} e^i$$
$$= \frac{1}{2}\sum_{i=1}^{M}\sum_{j=1, j\neq i}^{M} g_r\left(\|x^i - x^j\|\right)\|x^i - x^j\|^2.$$

Substituting the values of A and B in the $\dot{V}$ equation and after some cancellations we have

$$\dot{V} = -aM\sum_{i=1}^{M}\|e^i\|^2 + \frac{1}{2}\sum_{i=1}^{M}\sum_{j=1, j\neq i}^{M} g_r\left(\|x^i - x^j\|\right)\|x^i - x^j\|^2 - \sum_{i=1}^{M}\nabla_{x^i}\sigma^{\top}(x^i)(x^i - c_\sigma).$$

Then, from condition *ii)* above we have

$$\dot{V} \leq -aM\sum_{i=1}^{M}\|e^i\|^2 + \frac{1}{2}M(M-1)b - \sum_{i=1}^{M}\nabla_{x^i}\sigma^{\top}(x^i)(x^i - c_\sigma).$$

Now, note that the third term on the right hand side of the above equation (which we denote with C below) depends on the (gradient of the) profile and can be both negative and positive. For different profiles we have

- **plane**:

$$\nabla_{x^i}\sigma^{\top}(x^i) = 0 \Rightarrow C = \sum_{i=1}^{M}\nabla_{x^i}\sigma^{\top}(x^i)(x^i - c_\sigma) = 0.$$

- **quadratic**:

$$\nabla_{x^i}\sigma^{\top}(x^i) = A_\sigma(x^i - c_\sigma)^{\top} \Rightarrow C = A_\sigma\sum_{i=1}^{M}\|x^i - c_\sigma\|^2.$$

- **Gaussian**:

$$\nabla_{x^i}\sigma^{\top}(x^i) = \frac{A_\sigma}{l_\sigma}\exp\left(-\frac{\|x^i - c_\sigma\|^2}{l_\sigma}\right)(x^i - c_\sigma)^{\top} \Rightarrow$$
$$C = \frac{A_\sigma}{l_\sigma}\sum_{i=1}^{M}\|x^i - c_\sigma\|^2\exp\left(-\frac{\|x^i - c_\sigma\|^2}{l_\sigma}\right).$$

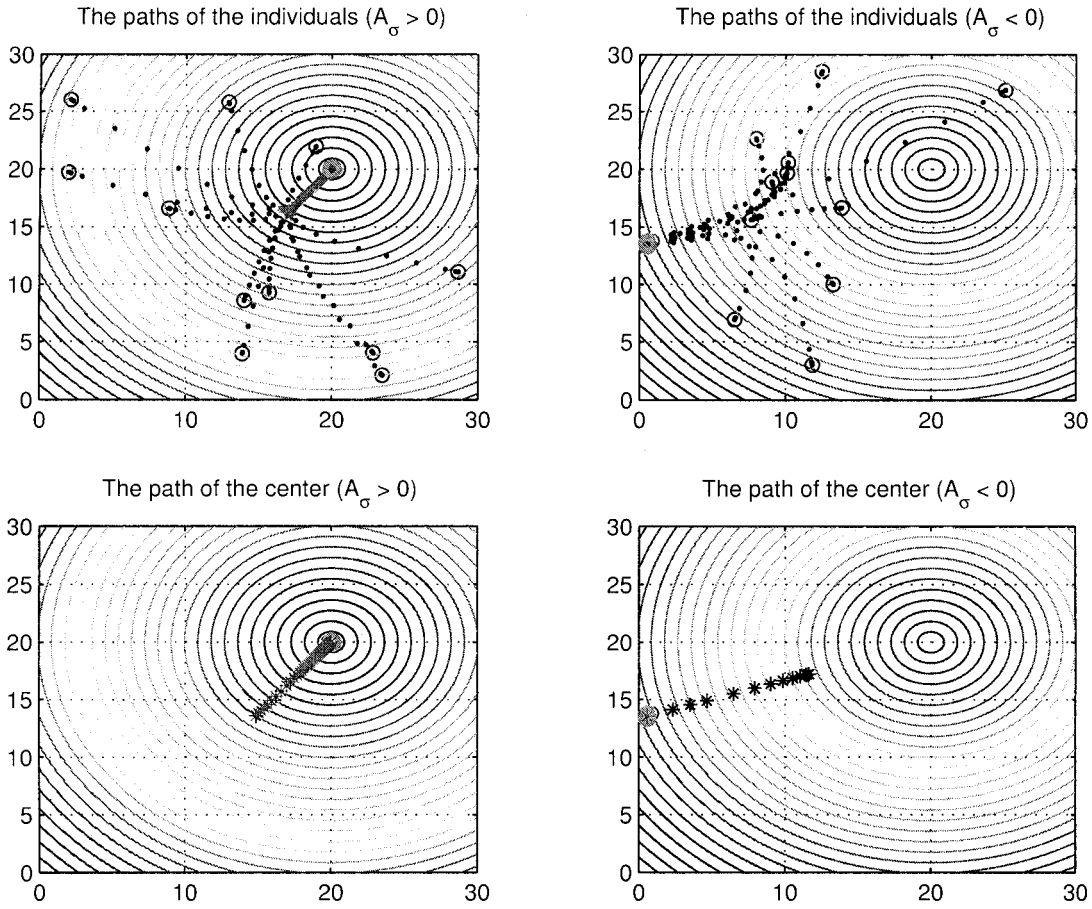

Fig. 2. Response for a quadratic profile.

- **multimodal Gaussian**:

$$\nabla_{x^i}\sigma^{\top}(x^i) = \sum_{j=1}^{N} \frac{A_\sigma^j}{l_\sigma^j} \exp\left(-\frac{\left\|x^i - c_\sigma^j\right\|^2}{l_\sigma^j}\right)\left(x^i - c_\sigma^j\right)^{\top} \Rightarrow$$

$$C = \sum_{i=1}^{M}\left(x^i - c_\sigma^k\right)^{\top} \sum_{j=1}^{N} \frac{A_\sigma^j}{l_\sigma^j}\left(x^i - c_\sigma^j\right) \times \exp\left(-\frac{\left\|x^i - c_\sigma^j\right\|^2}{l_\sigma^j}\right);$$

for some $1 \le k \le N$.

Consider the cases in which we have $A_\sigma > 0$ for the quadratic and Gaussian profiles, and $A_\sigma^k > 0$ for the multimodal Gaussian profile (i.e., the attractant profile cases). Then, the last term in the $\dot{V}$ equation is nonpositive for the first three profiles, namely the plane, quadratic and the gaussian profiles. For the multimodal Gaussian profile after some tedious but straightforward manipulation it is guaranteed to be nonpositive provided that the condition

$$\frac{A_\sigma^k}{l_\sigma^k}\left\|x^i - c_\sigma^k\right\| \exp\left(-\frac{\left\|x^i - c_\sigma^k\right\|^2}{l_\sigma^k}\right) \ge \sum_{j=1, j\neq k}^{N} \frac{\left|A_\sigma^j\right|}{l_\sigma^j}\left\|x^i - c_\sigma^j\right\| \exp\left(-\frac{\left\|x^i - c_\sigma^j\right\|^2}{l_\sigma^j}\right) \quad (9)$$

is satisfied for all i. Note that this condition is very similar to the condition in Lemma 4. Then, for these cases we can deduce that as $t \to \infty$ we will have

$$\frac{1}{M-1}\sum_{i=1}^{M}\|e^i\|^2 \le \frac{b}{2a}.$$

In other words, for the *root-mean-square* of the distances of the individuals to the center we have

$$e_{rms} = \sqrt{\frac{1}{M}\sum_{i=1}^{M}\|e^i\|^2} \le \sqrt{\frac{b}{2a}}$$

which is smaller than the bounds found in Lemma 1. Therefore, we have proved the following result.

Lemma 5: Consider the swarm described by the model in (1) with an attraction/repulsion function $g(\cdot)$ as given in (2) with linear attraction and (possibly unbounded) repulsion satisfying $g_r(\|x^i - x^j\|) \le (b)/(\|x^i - x^j\|^2)$, for some $b > 0$. Assume that the σ-profile is one of the following.

- A plane profile in (5).
- A quadratic profile in (6) with $A_\sigma > 0$.
- A Gaussian profile in (7) with $A_\sigma > 0$.
- A multimodal Gaussian profile in (8) with the condition in (9) satisfied for some k with $A_\sigma^k > 0$ and for all i.

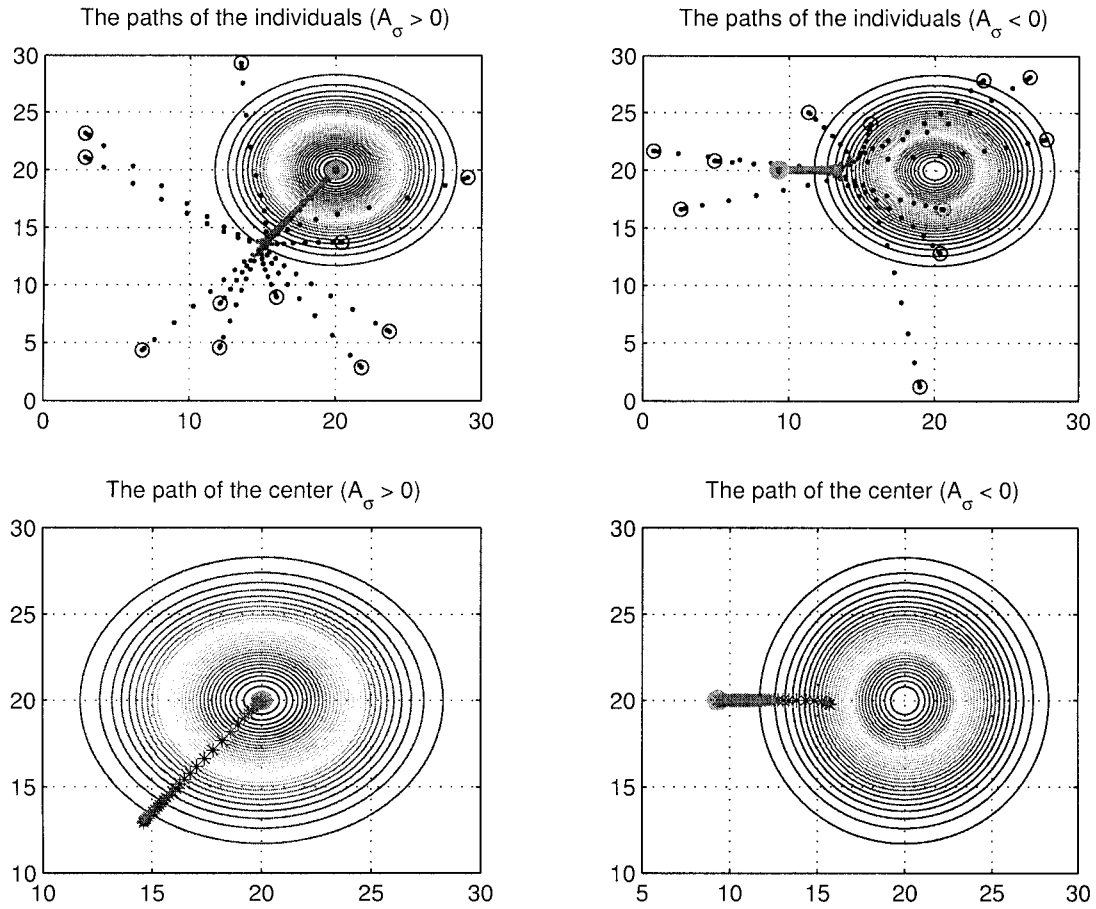

Fig. 3. Response for a Gaussian profile.

Then, as $t \to \infty$ we will have

$$e_{rms} \leq \sqrt{\frac{b}{2a}}.$$

One issue to note here is that the above result holds for all repulsion functions satisfying condition *ii)* above. Therefore, it holds also for the bounded repulsion functions considered earlier. The advantage of having unbounded repulsion functions is that they guarantee the avoidance of collision, as mentioned before.

Note also that if we had kept the negative third term in the derivative of the Lyapunov equation above, then the condition obtained for the negative definiteness of $\dot{V}$ would suggest a bound on the distance of the center $\bar{x}$ to the minimum c_σ (or c_σ^k in the multimodal Gaussian case). However, this bound is not necessarily small. Nevertheless, all the results for different profiles obtained in the preceding sections still hold (with appropriate modifications on the bounds on the swarm size) even with the new unbounded repulsion functions.

Finally, note that for the cases excluded in the theorem we cannot guarantee the same bounds. However, it is possible to derive bounds (which may be slightly larger) for these cases too. For example, one can show that for the Gaussian case with $A_\sigma < 0$ we will have

$$\varepsilon_{rms} = \sqrt{\frac{b}{2a} + \frac{|A_\sigma|}{aM}\exp(-1)}.$$

IX. Analysis of Individual Behavior in a Cohesive Swarm

The results in the previous sections specify whether the swarm will diverge or converge, and if it converges they specify in which regions of the profile it will converge, together with bounds on the swarm size. The results above do not provide information about the ultimate behavior of the individuals. In other words, they do not specify whether the individuals will eventually stop moving or will end up in oscillatory motions within the specified regions. In this section, we will investigate the ultimate behavior of the individuals. In particular, we will analyze the ultimate behavior of the individuals in a quadratic profile with $A_\sigma > 0$, a Gaussian profile with $A_\sigma > 0$, and in a multimodal Gaussian profile with the conditions of Lemma 4 for the $A_\sigma^k > 0$ case satisfied. To this end, first, we define the state x of the system as the vector of the positions of the swarm members $x = [x^{1\top}, \ldots, x^{M\top}]^\top$. Let the invariant set of equilibrium points be

$$\Omega_e = \{x : \dot{x} = 0\}.$$

We will prove that for the above mentioned cases as $t \to \infty$ the state $x(t)$ converges to Ω_e, i.e., eventually all the individuals stop moving.

Theorem 4: Consider the swarm described by the model in (1) with an attraction/repulsion function $g(\cdot)$ as given in (2) with

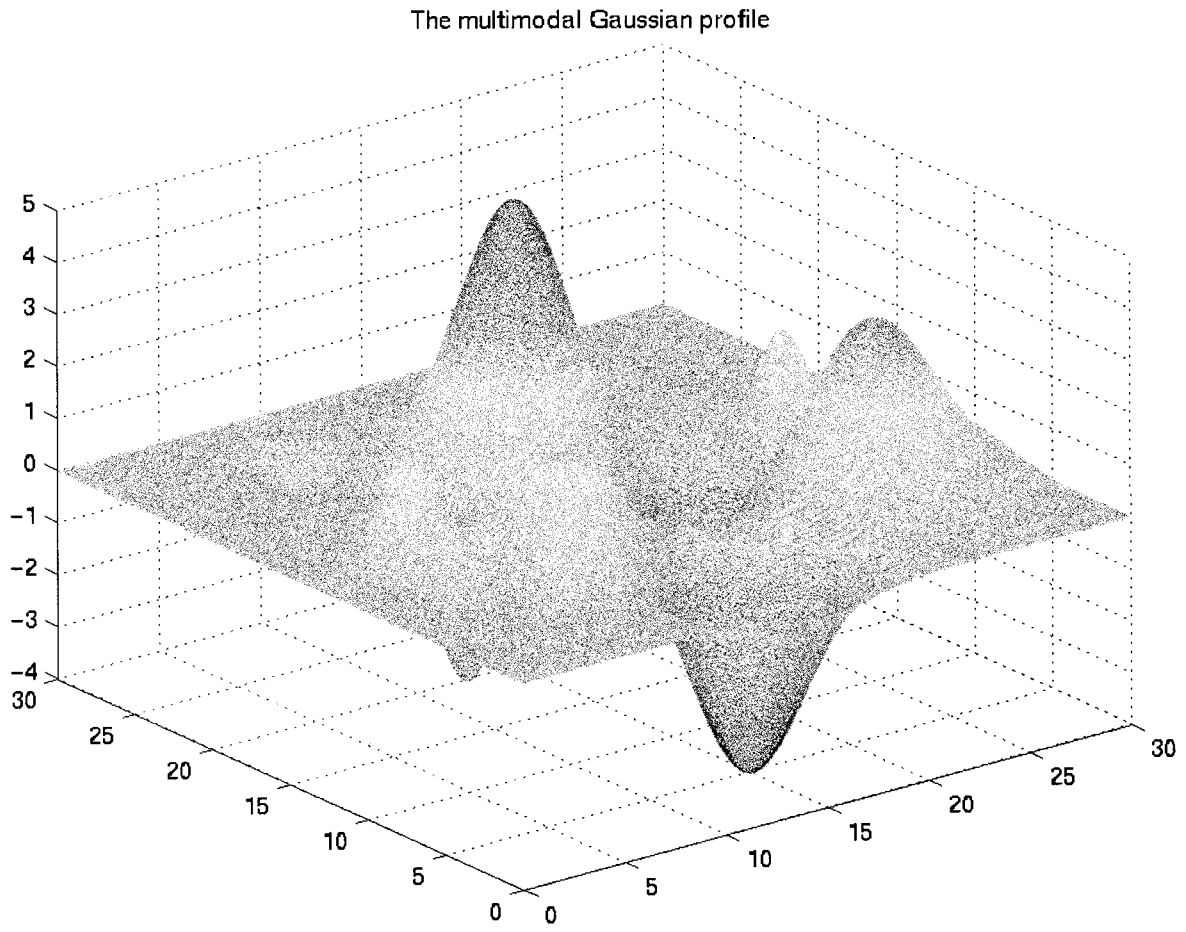

Fig. 4. Multimodal Gaussian profile.

linear attraction and bounded repulsion. Assume that the σ-profile is one of the following.

- A quadratic profile in (6) with $A_\sigma > 0$.
- A Gaussian profile in (7) with $A_\sigma > 0$.
- A multimodal Gaussian profile in (8) with conditions of Lemma 4 for the $A_\sigma^k > 0$ case satisfied.

Then, as $t \to \infty$ we have the state $x(t) \to \Omega_e$.

Proof: Choose the generalized Lyapunov function $J(x)$ as the total artificial potential energy E in the system. In other words, choose $J(x)$ as

$$J(x)=\sum_{i=1}^{M}\sigma(x^i)+\frac{1}{2}\sum_{i=1}^{M-1}\sum_{j=i+1}^{M}\left[a\|x^i-x^j\|^2-J_r\left(\|x^i-x^j\|\right)\right]$$

whose gradient at x^i is

$$\nabla_{x^i}J(x)=\nabla_{x^i}\sigma(x^i)+\sum_{j=1,j\neq i}^{M}(x^i-x^j)\times\left[a-g_r\left(\|x^i-x^j\|\right)\right]=-\dot{x}^i$$

and its time derivative is given by

$$\dot{J}(x)=\left[\nabla_x J(x)\right]^\top\dot{x}=\sum_{i=1}^{M}\left[\nabla_{x^i}J(x)\right]^\top\dot{x}^i=-\sum_{i=1}^{M}\|\dot{x}^i\|^2\leq 0$$

for all $t \geq 0$. Now, note that for all the cases in the hypothesis of the theorem, we have $J(x)$ bounded from below and the set

$$\Omega_c=\{x : J(x)\leq J\left(x(0)\right)\}$$

is compact and positively invariant with respect to the motions of the system. Then, we can apply the LaSalle's Invariance Principle from which we conclude that as $t \to \infty$ the state x converges to the largest invariant subset of the set $\Omega \subset \Omega_c$ defined as

$$\Omega=\left\{x : \dot{J}(x)=0\right\}=\{x : \dot{x}=0\}=\Omega_e.$$

Since each point in Ω_e is an equilibrium, Ω_e is an invariant set and this proves the result. ■

One issue to note here is that for the cases excluded in the above theorem, i.e., for the plane profile, quadratic profile with $A_\sigma < 0$, Gaussian profile with $A_\sigma < 0$, and the multimodal Gaussian profile for $A_\sigma^k < 0$ case or not necessarily satisfying the conditions of Lemma 4, the set Ω_c may not be compact. Therefore, we cannot apply the LaSalle's Invariance Principle. Moreover, since they are (possibly) diverging, intuitively we do not expect them to stop their motion. Furthermore, note that for the plane profile we have $\Omega_e = \emptyset$. In other words, there is no equilibrium for the swarm moving in a plane profile.

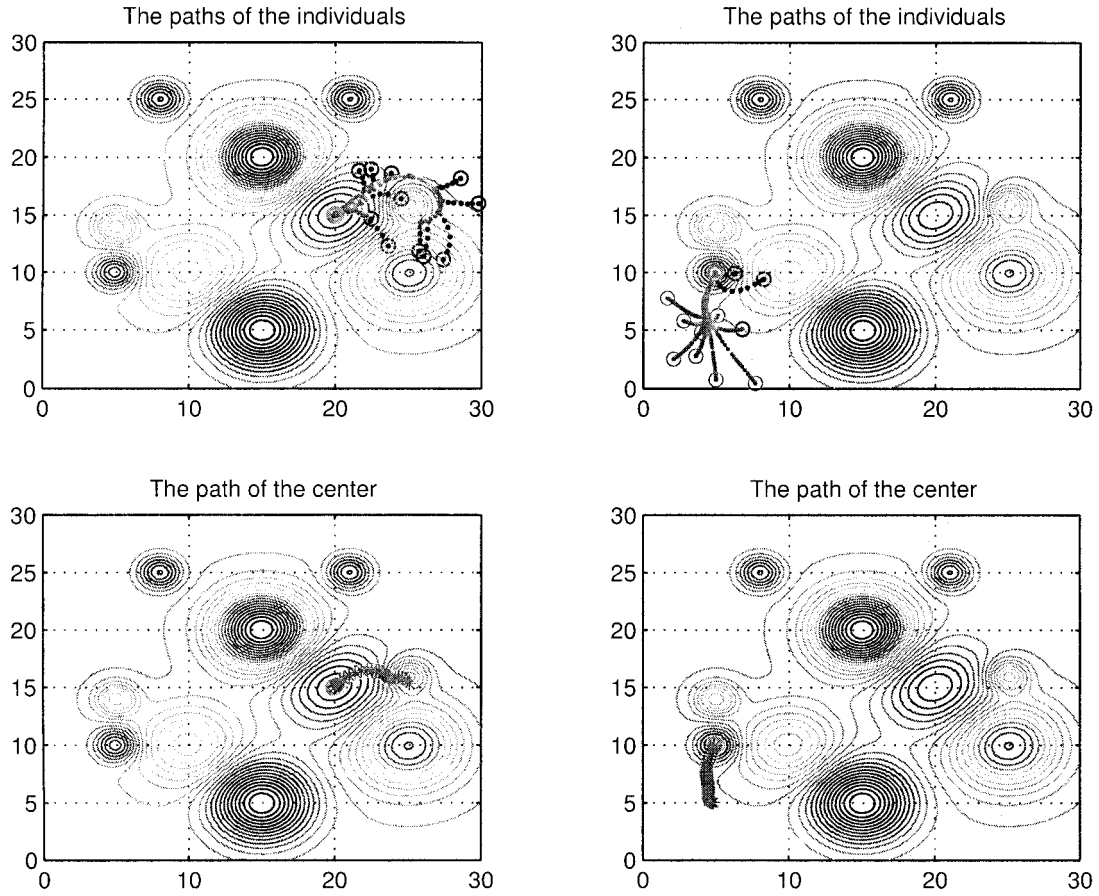

Fig. 5. Response for a multimodal Gaussian profile (initial positions close to a minimum).

X. Simulation Examples

In this section, we will provide some simulation examples to illustrate the theory developed in the preceding sections. We chose an $n = 2$ dimensional space for ease of visualization of the results and used the region [0, 30] $\times$ [0, 30] in the space. In all the simulations performed below we used $M = 11$ individuals. As parameters of the attraction/repulsion function $g(\cdot)$ in (2) we used $a = 0.01$, $b = 0.4$, and $c = 0.01$ for most of the simulations and $a = 0.1$ for some of them. We performed simulations for all the profiles discussed in this article.

The first result shown in Fig. 1 is for a plane profile with $a_\sigma = [0.1, 0.2]^\top$ for the plots on the left and $a_\sigma = [0.5, 1]^\top$ for those on the right. One easily can see that in both of the cases, as expected, the swarm moves along the negative gradient $-a_\sigma$ exiting the simulation region toward unboundedness. Note that initially for the case $a_\sigma = [0.1, 0.2]^\top$ some of the individuals move in a direction opposite to the negative gradient. This is because the inter-individual attraction is much stronger than the intensity of the profile. In contrast, for the $a_\sigma = [0.5, 1]^\top$ case, the intensity of the profile is high enough to dominate the inter-individual attraction. This, of course, does not mean that the swarm will not aggregate. As they move they will eventually aggregate as was shown in the preceding sections. We also show the plots of the swarm centers. Note that the motion of the centers is similar for both of the cases as expected from the analysis in the preceding sections.

The next result is for the quadratic profile as shown in Fig. 2. We chose a profile with extremum at $c_\sigma = [20, 20]^\top$ and magnitude $A_\sigma = \pm 0.02$. The two plots on the left of the figure show the paths of the individuals and the center of the swarm for the case $A_\sigma > 0$, whereas those on the right are for the $A_\sigma < 0$ case. Once more, we observe that the results support the analysis of preceding sections. Note also that the center $\bar{x}$ of the swarm converges to the minimum of the profile c_σ for the $A_\sigma > 0$ case and diverges from the maximum for the $A_\sigma < 0$ case.

Results of a similar nature were obtained also for the Gaussian profile as shown in Fig. 3. Once more we chose $c_\sigma = [20, 20]^\top$ as the extremum of the profile. The other parameters of the profile were chosen to be $A_\sigma = \pm 2$ and $l_\sigma = 20$. Note that for the $A_\sigma > 0$ case, even though in theory we could not prove that $\bar{x}(t) \to c_\sigma$, in simulations we observe that this is apparently the case. This was happening systematically in all the simulations that we performed.

In the simulation examples for the multimodal Gaussian profile we used the profile shown in Fig. 4, which has several minima and maxima. The global minimum is located at $[15, 5]^\top$ with a magnitude of 4 and a spread of 10. The plot in Fig. 5 shows two example runs with initial member positions nearby a local minimum and show convergence of the entire swarm to that minimum. The attraction parameter a was chosen to be

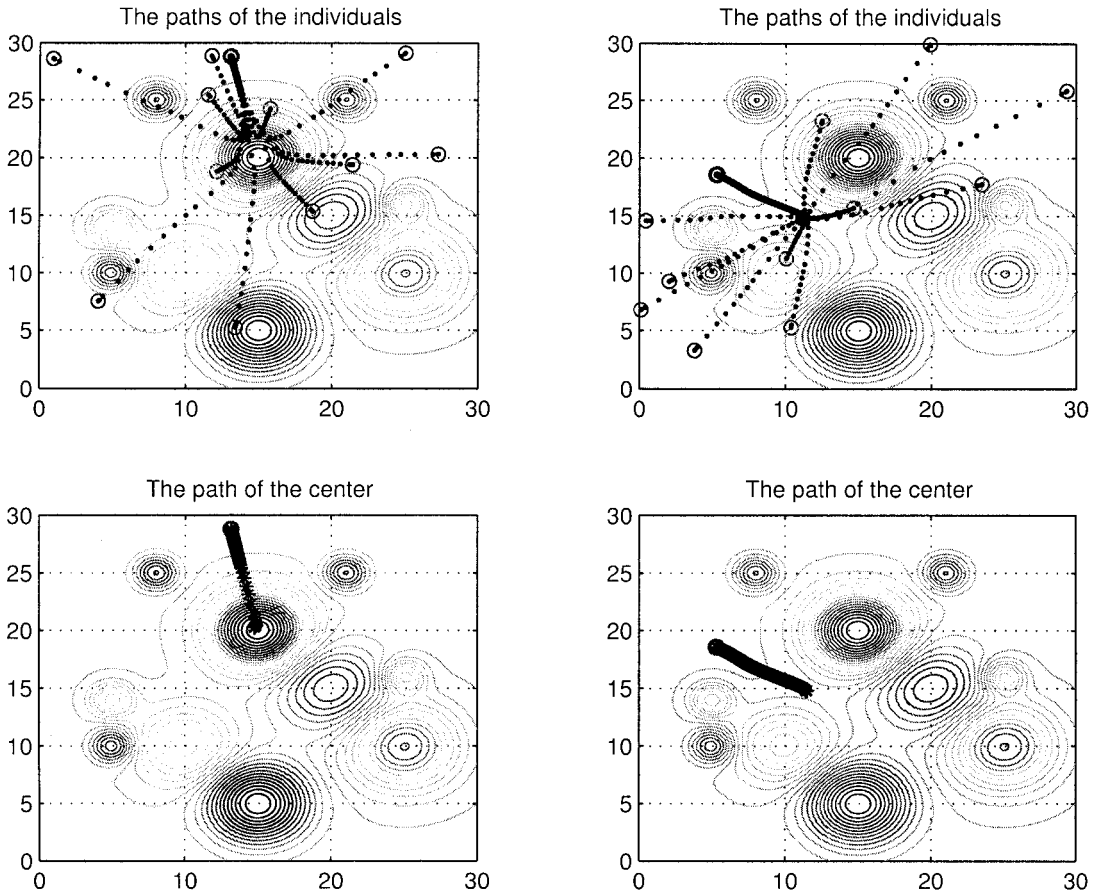

Fig. 6. Response for a multimodal Gaussian profile ($a = 0.1$).

$a = 0.01$ for this case. Fig. 6, on the other hand, illustrates the case in which we increased the attraction parameter to $a = 0.1$. You can see that the attraction is so strong that the individuals climb gradients to form a cohesive swarm. For this and similar cases, the manner in which the overall swarm will behave (where it will move) depends on the initial position of the center $\bar{x}$ of the swarm. For these two runs the center happened to be located on regions which caused the swarm to diverge. For some other simulation runs (not presented here) with different initial conditions the entire swarm converges to either a local or global minima. Fig. 7 shows two runs for which we decreased the attraction parameter again to $a = 0.01$ and initialized the swarm member positions all over the region. For both of the simulations you can see that the swarm fails to form a cohesive cluster since the initial positions of the individuals are such that they move to a nearby local minima and the attraction is not strong enough to "pull them out" of these valleys. This causes formation of several groups or clusters of individuals at different locations of the space. For these reasons, the center $\bar{x}$ of the swarm does not converge to any minimum. Note, however, that this is expected since for this case the conditions of Theorem 3 are not satisfied. Nevertheless, the result of Lemma 1 still holds. The only issue is that ε_{mG} is large and contains all the region within which all the individuals eventually remain. Finally, note also that during their motion to the groups, the individuals try to avoid climbing gradients and this results in motions resembling the motion of individuals in real biological swarms.

XI. Conclusion

In this article, we developed a simple model of swarming in the presence of an attractant/repellent profile and analyzed its stability properties for different profiles. Our model can be viewed as a model for stable social foraging of swarms in a profile of nutrients. We showed collective convergence to more favorable regions of the profile (i.e., the regions with higher concentration of nutrients) and diverge from unfavorable regions (i.e., the regions with higher concentration of toxic substances). The bounds on the swarm size and the distance of the swarm center from the minimum points of the profile illustrate the basic concepts in foraging theory of balance between the desire to stay with the swarm and the desire to find more food. Note that the model that we presented here directly addresses the problem of coordination of agents and interactions with the environment based on simple potentials. Therefore, even though we get our inspiration from biology, we believe that our work is a contribution to the multi-agent coordination literature. In fact, note that in some applications, such as undersea explorations by a group of robots, the agents may need to follow the gradient of some substance [36], which is the problem considered here, and the results of this article are directly applicable.

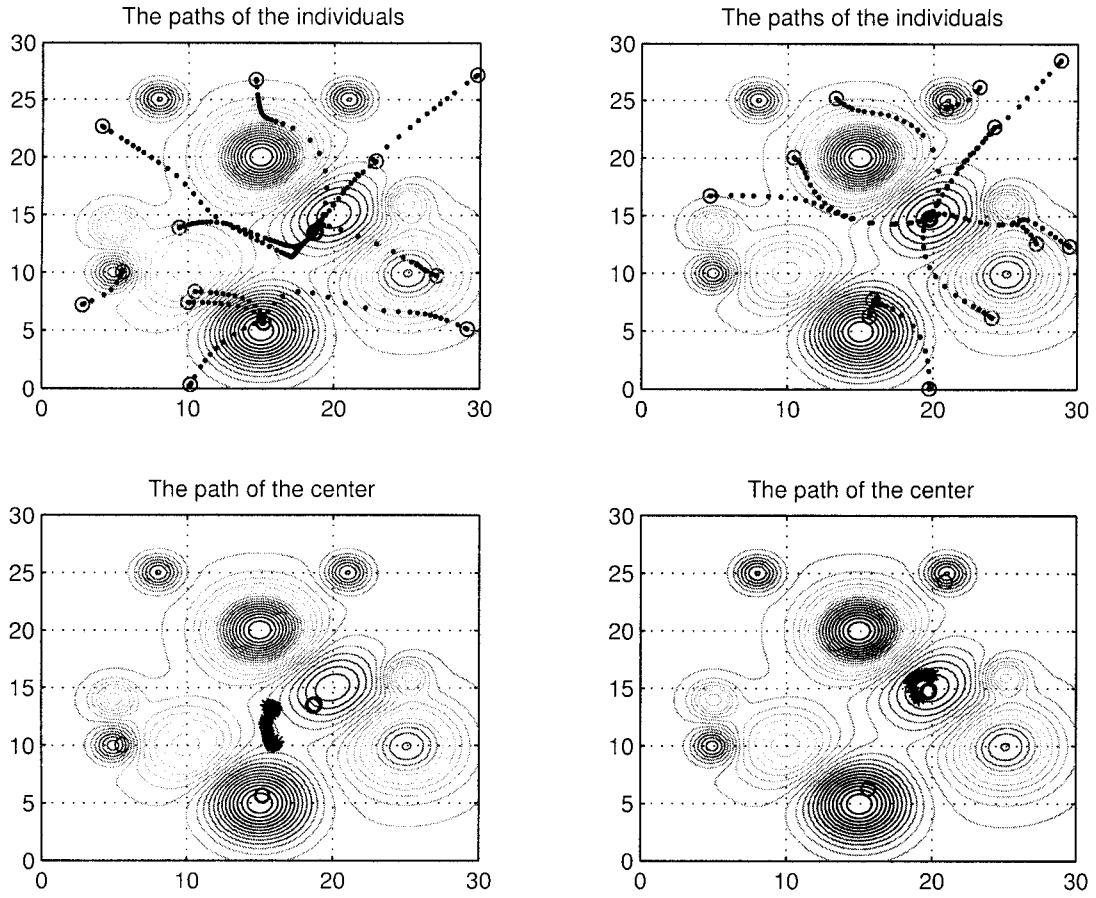

Fig. 7. Response for a multimodal Gaussian profile ($a = 0.01$).

Our model is essentially a kinematic model illustrating and providing proof for multi-agent aggregation. It can serve as a starting point for engineers who need to design a multi-agent system that posesses such characteristics. For example, the trajectories generated by our model can be used as reference trajectories for robots (or other agents) to follow/track if there is a need for a group of robots to perform aggregating behavior in an environment containing targets and threats/obstacles. For this case, the threats (to be avoided) are analogous to the toxic substances and the targets (to be moved toward) are analogous to food. Then, the problem of the system designer is reduced to developing a controller to guarantee trajectory following given the specific (actual) robot dynamics. For this reason, our results in this article serve as a "proof of concept" for such operation—an aggregating behavior of agents moving in an environment with targets and obstacles. Note also that the swarm model discussed here can be viewed as performing distributed optimization using a distributed gradient method.

As pointed out in [23] foraging has important relations to control and automation. Foraging strategies in biological creatures have been "designed" and "tested" by evolution for millions of years. By studying, understanding, and modeling such behavior we may be able to gain ideas for developing distributed coordination and control strategies for cooperative team behavior of multi-agent robotic systems such as unmanned undersea, land or air vehicles. For example, there is a growing interest in the development of distributed coordination and control strategies for uninhabited autonomous air vehicles (UAAVs) [23] moving on a landscape where there are mobile threats/targets each with "target priority" and "thread severity." Such a problem can clearly be viewed as a foraging problem (although not of the type discussed in this article), and the ideas from social foraging of biological creatures can be helpful for solving it. In the light of this, the results in this article can be viewed as an initial step toward developing a comprehensive theory for stable social foraging of swarms as well as transferring the ideas from social foraging to the control literature.

Possible future extensions of the work here could be extension to the case of time-varying attractant/repellent profiles. In engineering context this will correspond to a dynamically changing environment or environment containing moving targets or threats (a very relevant and important problem). Another possible extension is to consider swarm members (or agents) which have limited sensing range and analyze stability (cohesion) under these conditions. For such a model it may be possible to prove (under some conditions) local stability (cohesion) results. The emergent behavior of such a model will (probably) be biologically more realistic.

REFERENCES

[1] D. Grünbaum, "Schooling as a strategy for taxis in a noisy environment," in *Animal Groups in Three Dimensions*, J. K. Parrish and W. M. Hamner, Eds. Cambridge, U.K.: Cambridge Univ. Press, 1997, pp. 257–281.

[2] ——, "Schooling as a strategy for taxis in a noisy environment," *Evolutionary Ecol.*, vol. 12, pp. 503–522, 1998.

[3] C. M. Breder, "Equations descriptive of fish schools and other animal aggregations," *Ecology*, vol. 35, no. 3, pp. 361–370, 1954.

[4] K. Warburton and J. Lazarus, "Tendency-distance models of social cohesion in animal groups," *J. Theoretical Biol.*, vol. 150, pp. 473–488, 1991.

[5] A. Okubo, "Dynamical aspects of animal grouping: swarms, schools, flocks, and herds," *Adv. Biophys.*, vol. 22, pp. 1–94, 1986.

[6] D. Grünbaum and A. Okubo, "Modeling social animal aggregations," in *Frontiers in Theoretical Biology*. New York: Springer-Verlag, 1994, vol. 100, pp. 296–325.

[7] A. Mogilner and L. Edelstein-Keshet, "A nonlocal model for a swarm," *J. Math. Biol.*, vol. 38, pp. 534–570, 1999.

[8] R. Durrett and S. Levin, "The importance of being discrete (and spatial)," *Theoretical Pop. Biol.*, vol. 46, pp. 363–394, 1994.

[9] S. Gueron and S. A. Levin, "The dynamics of group formation," *Math Biosci.*, vol. 128, pp. 243–264, 1995.

[10] J. K. Parrish, S. V. Viscido, and D. Grünbaum, "Self-organized fish school: an examination of emergent properties," *Biol. Bull.*, vol. 202, pp. 296–305, June 2002.

[11] J. K. Parrish and W. M. Hamner, Eds., *Animal Groups in Three Dimensions*. Cambridge, U.K.: Cambridge University Press, 1997.

[12] S. Camazine, J.-L. Deneubourg, N. R. Franks, J. Sneyd, G. Theraulaz, and E. Bonabeau, *Self-Organization in Biological Systems*. Princeton, NJ: Princeton Univ. Press, Apr. 2001.

[13] L. Edelstein-Keshet, *Mathematical Models in Biology*. New York: Random House, 1989.

[14] J. D. Murray, *Mathematical Biology*. New York: Springer-Verlag, 1989.

[15] T. Vicsek, A. Czirok, E. Ben-Jacob, I. Cohen, and O. Shochet, "Novel type of phase transition in a system of self-driven particles," *Phys. Rev. Lett.*, vol. 75, no. 6, pp. 1226–1229, Aug. 1995.

[16] A. Czirok, E. Ben-Jacob, I. Cohen, and T. Vicsek, "Formation of complex bacterial colonies via self-generated vortices," *Phys. Rev. E.*, vol. 54, no. 2, pp. 1791–1801, Aug. 1996.

[17] A. Czirok, H. E. Stanley, and T. Vicsek, "Spontaneously ordered motion of self-propelled particles," *J. Phys. A: Math Nucl. General*, vol. 30, pp. 1375–1385, 1997.

[18] A. Czirok and T. Vicsek, "Collective behavior of interacting self-propelled particles," *Physica A*, vol. 281, pp. 17–29, 2000.

[19] N. Shimoyama, K. Sugawa, T. Mizuguchi, Y. Hayakawa, and M. Sano, "Collective motion in a system of motile elements," *Phys. Rev. Lett.*, vol. 76, no. 20, pp. 3870–3873, May 1996.

[20] H. Levine and W.-J. Rappel, "Self-organization in systems of self-propelled particles," *Phys. Rev. E*, vol. 63, no. 1, pp. 017 101-1–017 101-4, January 2001.

[21] D. W. Stephens and J. R. Krebs, *Foraging Theory*. Princeton, NJ: Princeton Univ. Press, 1986.

[22] E. Bonabeau, M. Dorigo, and G. Theraulaz, *Swarm Intelligence: From Natural to Artificial Systems*. New York: Oxford Univ. Press, 1999.

[23] K. M. Passino, "Biomimicry of bacterial foraging for distributed optimization and control," *IEEE Control Syst. Mag.*, vol. 22, pp. 52–67, June 2002.

[24] J. Kennedy and R. C. Eberhart, *Swarm Intelligence*. San Mateo, CA: Morgan Kaufmann, 2001.

[25] M. Clerc and J. Kennedy, "The particle swarm—explosion, stability, and convergence in a multidimensional complex space," *IEEE Trans. Evolutionary Computat.*, vol. 6, pp. 58–73, Feb. 2002.

[26] M. M. Polycarpou, Y. Yang, and K. M. Passino, "Cooperative control of distributed multi-agent systems," *IEEE Control Syst. Mag.*, to be published.

[27] F. Giulietti, L. Pollini, and M. Innocenti, "Autonomous formation flight," *IEEE Control Syst. Mag.*, vol. 20, pp. 34–44, Dec. 2000.

[28] T. Balch and R. C. Arkin, "Behavior-based formation control for multirobot teams," *IEEE Trans. Robot. Automat.*, vol. 14, pp. 926–939, Dec. 1998.

[29] I. Suzuki and M. Yamashita, "Distributed anonymous mobile robots: formation of geometric patterns," *SIAM J. Comput.*, vol. 28, no. 4, pp. 1347–1363, 1999.

[30] H. Yamaguchi, "A cooperative hunting behavior by mobile-robot troops," *Int. J. Robot. Res.*, vol. 18, pp. 931–940, Sept. 1999.

[31] J. H. Reif and H. Wang, "Social potential fields: a distributed behavioral control for autonomous robots," *Robot. Auton. Syst.*, vol. 27, pp. 171–194, 1999.

[32] J. P. Desai, J. Ostrowski, and V. Kumar, "Controlling formations of multiple mobile robots," in *Proc. IEEE Int. Conf. Robot. Automat.*, Leuven, Belgium, May 1998, pp. 2864–2869.

[33] M. Egerstedt and X. Hu, "Formation constrained multi-agent control," *IEEE Trans Robot. Automat.*, vol. 17, pp. 947–951, Dec. 2001.

[34] P. Ögren, M. Egerstedt, and X. Hu, "A control Lyapunov function approach to multi-agent coordination," in *Proc. Conf. Decision Contr.*, Orlando, FL, Dec. 2001, pp. 1150–1155.

[35] N. E. Leonard and E. Fiorelli, "Virtual leaders, artificial potentials and coordinated control of groups," in *Proc. Conf. Decision Contr.*, Orlando, FL, Dec. 2001, pp. 2968–2973.

[36] R. Bachmayer and N. E. Leonard, "Vehicle networks for gradient descent in a sampled environment," in *Proc. Conf. Decision Contr.*, Las Vegas, NV, Dec. 2002, pp. 112–117.

[37] K. Jin, P. Liang, and G. Beni, "Stability of synchronized distributed control of discrete swarm structures," in *Proc. IEEE Int. Conf. Robot. Automat.*, San Diego, CA, May 1994, pp. 1033–1038.

[38] G. Beni and P. Liang, "Pattern reconfiguration in swarms—convergence of a distributed asynchronous and bounded iterative algorithm," *IEEE Trans. Robot. Automat.*, vol. 12, pp. 485–490, June 1996.

[39] Y. Liu, K. M. Passino, and M. Polycarpou, "Stability analysis of one-dimensional asynchronous swarms," in *Proc. Amer. Contr. Conf.*, Arlington, VA, June 2001, pp. 716–721.

[40] ——, "Stability analysis of one-dimensional asynchronous mobile swarms," in *Proc. Conf. Decision Contr.*, Orlando, FL, Dec. 2001, pp. 1077–1082.

[41] Y. Liu, K. M. Passino, and M. M. Polycarpou, "Stability analysis of one-dimensional asynchronous swarms," IEEE Trans. Automat. Contr., 2003, to be published.

[42] V. Gazi and K. M. Passino, "Stability of a one-dimensional discrete-time asynchronous swarm," in *Proc. Joint IEEE Int. Symp. Intell. Contr./IEEE Conf. Contr. Applicat.*, Mexico City, Mexico, Sept. 2001, pp. 19–24.

[43] D. P.Dimitri P. Bertsekas and J. N.John N. Tsitsiklis, *Parallel and Distributed Computation: Numerical Methods*. Belmont, MA: Athena Scientific, 1997.

[44] J. Bender and R. Fenton, "On the flow capacity of automated highways," *Transport. Sci.*, vol. 4, pp. 52–63, Feb. 1970.

[45] D. Swaroop, J. K. Hedrick, C. C. Chien, and P. Ioannou, "A comparison of spacing and headway control laws for automatically controlled vehicles," *Vehicle Syst. Dyn.*, vol. 23, pp. 597–625, 1994.

[46] S. Darbha and K. R. Rajagopal, "Intelligent cruise control systems and traffic flow stability," *Transport. Res. C*, vol. 7, pp. 329–352, 1999.

[47] Y. Liu, K. M. Passino, and M. M. Polycarpou, "Stability analysis of m-dimensional asynchronous swarms with a fixed communication topology," in *Proc. Amer. Contr. Conf.*, Anchorage, AK, May 2002, pp. 1278–1283.

[48] ——, "Stability analysis of m-dimensional asynchronous swarms with a fixed communication topology," *IEEE Trans. Automat. Contr.*, vol. 48, pp. 76–95, Jan. 2003.

[49] V. Gazi and K. M. Passino, "Stability analysis of swarms," in *Proc. Amer. Contr. Conf.*, Anchorage, AK, May 2002, pp. 1813–1818.

[50] ——, "Stability analysis of swarms," *IEEE Trans. Automat. Contr.*, vol. 48, pp. 692–697, Apr. 2003.

[51] ——, "A class of attraction/repulsion functions for stable swarm aggregations," in *Proc. Conf. Decision Contr.*, Las Vegas, NV, Dec. 2002, pp. 2842–2847.

[52] O. Khatib, "Real-time obstacle avoidance for manipulators and mobile robots," *Int. J. Robot. Res.*, vol. 5, no. 1, pp. 90–98, 1986.

[53] E. Rimon and D. E. Koditschek, "Exact robot navigation using artificial potential functions," *IEEE Trans. Robot. Automat.*, vol. 8, pp. 501–518, Oct. 1992.

[54] V. Gazi and K. M. Passino, "Stability analysis of swarms in an environment with an attractant/repellent profile," in *Proc. Amer. Contr. Conf.*, Anchorage, AK, May 2002, pp. 1819–1824.

[55] ——, "Stability analysis of social foraging swarms: combined effects of attractant/repellent profiles," in *Proc. Conf. Decision Contr.*, Las Vegas, NV, Dec. 2002, pp. 2848–2853.

[56] B. L. Partridge, "The structure and function of fish schools," *Sci. Amer.*, vol. 245, pp. 114–123, 1982.

[57] S. Gueron, S. A. Levin, and D. I. Rubenstein, "The dynamics of herds: from individuals to aggregations," *J. Theoretical Biol.*, vol. 182, pp. 85–98, 1996.

[58] H. K. Khalil, *Nonlinear Systems*, 2nd ed. Upper Saddle River, NJ: Prentice-Hall, 1996.

Veysel Gazi (M'03) received the B.S. degree in electrical and electronics engineering from Middle East Technical University, Ankara, Turkey, in 1996 and the M.S. and Ph.D. degrees in electrical engineering from Ohio State University, Columbus, in 1998 and 2002, respectively.

From September 1996 to May 1997, he was supported by The Scientific and Technical Research Council of Turkey (TÜBITAK), and from May 1997 to August 2002, he was a Research Associate at the Department of Electrical Engineering, Ohio State University. Currently he is an Assistant Professor at the Department of Electrical and Electronics Engineering, Atilim University, Ankara, Turkey. His current research interests include stability analysis of swarms as well as cooperative coordination and control of multi-agent systems.

Kevin M. Passino (S'79–M'90–SM'96) received the Ph.D. degree in electrical engineering from the University of Notre Dame, Notre Dame, IN, in 1989.

He has worked on control systems research at Magnavox Electronic Systems Co. and McDonnell Aircraft Co. He spent a year at Notre Dame as a Visiting Assistant Professor and is currently Professor of electrical engineering at Ohio State University, Columbus. Also, he is the Director of the OSU Collaborative Center of Control Science that is funded by AFRL/VA and AFOSR. He is co-editor of *An Introduction to Intelligent and Autonomous Control* (Boston, MA: Kluwer, 1993), co-author of *Fuzzy Control* (Reading, MA: Addison-Wesley, 1998), co-author of *Stability Analysis of Discrete Event Systems* (New York: Wiley, 1998), co-author of *The RCS Handbook: Tools for Real Time Control Systems Software Development* (New York: Wiley, NY, 2001), co-author of *Stable Adaptive Control and Estimation for Nonlinear Systems: Neural and Fuzzy Approximator Techniques* (New York: Wiley, 2002).

Dr. Passino was Associate Editor for the IEEE TRANSACTIONS ON AUTOMATIC CONTROL and the IEEE TRANSACTIONS ON FUZZY SYSTEMS. He was the Guest Editor for the 1993 *IEEE Control Systems Magazine Special Issue on Intelligent Control*; and a Guest Editor for a special track of papers on Intelligent Control for *IEEE Expert Magazine* in 1996; and was on the Editorial Board of the *International Journal for Engineering Applications of Artificial Intelligence*. He was the Vice President of Technical Activities, IEEE Control Systems Society (CSS), was an elected member of the IEEE Control Systems Society Board of Governors, and Chair for the IEEE CSS Technical Committee on Intelligent Control. He was a Program Chairman for the 8th IEEE International Symposium on Intelligent Control, 1993 and was the General Chair for the 11th IEEE International Symposium on Intelligent Control. He was the Program Chair of the 2001 IEEE Conference on Decision and Control. He is currently a Distinguished Lecturer for the IEEE Control Systems Society.